A

DISSERTATION REPORT

on

STIFFNESS CHARACTERISTICS OF SOFT ROCK JOINTS

Submitted to

DELHI COLLEGE OF ENGINEERING, DELHI

In partial fulfillment of the requirement for the Degree of

MASTER OF ENGINEERING

IN

STRUCTURAL ENGINEERING

Submitted By:

VIKAS VARSHNEY

(Roll No- 12387)

Under the supervision of:

Prof. A. Trivedi
Professor

Mr. A. K. Shrivastava
Lecturer

DEPARTMENT OF CIVIL ENGINEERING,

DELHI COLLEGE OF ENGINEERING

FACULTY OF TECHNOLOGY, UNIVERSITY OF DELHI

DELHI

2009

CERTIFICATE

This is to certify that the project entitled **"STIFFNESS CHARACTERISTICS OF SOFT ROCK JOINTS"** being submitted by me, is a bonafide record of my own work carried by me under the guidance and supervision of Prof. A. Trivedi and Mr. A.K. Shrivastava in partial fulfillment of requirements for the award of the degree of Master of Engineering (Structural Engineering) in civil engineering from university of Delhi, Delhi.

The matter embodied in this project has not been submitted for the award of any other degree.

VIKAS VARSHNEY
Roll No: 12387
University of Delhi
Date:
Place: New Delhi

This is certified that above statement made by the student is correct to the best of our knowledge.

Prof. A. Trivedi
Professor

Mr. A.K. Shrivastava
Lecturer

Department of Civil Engineering
Delhi College of Engineering
Faculty of Technology, University of Delhi
New Delhi – 110042

ACKNOWLEDGEMENT

I would like to express my sincere gratitude and profound sense to the esteemed supervisors **Prof. A. Trivedi** and **Mr. A. K. Shrivastava** for their able guidance and constant encouragement, timely tangible and copious comments without which this dissertation would not have been completed.

I would also like to express my gratitude towards **Prof. S. K. Singh,** Head, Department of CIVIL Engineering, and **Mr. R.K. Shukla**, Librarian, Delhi College of Engineering for providing conducive environment to facilitate this study.

I am also thankful to all the staff members of Concrete Technology Laboratory and Soil Mechanics Laboratory, and special thanks to Mr. Agnihotri, mechanic, soil mechanics lab who has been very cooperative.

I am greatly thankful to all my friends who helped me throughout the completion of this project.

I am deeply indebted to my family for their immense affection, encouragement and blessings at all stages of my life.

(VIKAS VARSHNEY)

ABSTRACT

The existence of one or several sets of discontinuities in a rock mass creates anisotropy in its response to loading and unloading. It is very much essential to understand the deformability of these rocks discontinuities. This is helpful for design of various structures and their foundations like tunnels, foundations of heavy structures like dams and tall buildings, abutments of arch dams and bridges and many underground structures. These deformation properties of rock joints can be described by stiffness characteristics. These characteristics are namely shear stiffness and normal stiffness. Shear stiffness of a rock joint can be estimated by conducting the direct shear test and the normal stiffness can be evaluated from the direct compression test. These stiffness characteristics are required to understand deformation in practice and also the same is required as an input by professional software for various analysis and design.

In this present work, an attempt has been made to predict the stiffness characteristics for two different types of joint profiles i.e naturally broken joint (Type I) and hacksaw tooth cut joint (Type II). The shear stiffness for both types of joints was estimated by conducting direct shear tests at various normal stress conditions. The normal stiffness for both types of joints was estimated using compressive strength test. Also the numbers of joints have been varied from 1 to 4, to find normal stiffness for both types of joints. Several tests have been done for estimation of stiffness characteristics.

It was observed that the shear stiffness increases with an increase in normal stress. Average normal stiffness values for Type I joints was lesser than average normal stiffness values for Type II joints. In addition to that, empirical equations have been proposed to estimate the shear stiffness of rock joints.

CONTENTS

LIST OF FIGURES

LIST OF TABLES

LIST OF NOTATIONS

A	=	Area of joint
c	=	Cohesion intercept
d_n	=	Peak dilation angle
D	=	Fractal dimension
f	=	Friction factor accounting for roughness of joint surface
g	=	Acceleration due to gravity
h	=	Depth
h_n	=	Dilation
i	=	Roughness angle or angle of asperity
JRC	=	Joint roughness coefficient
JCS	=	Joint wall compressive strength
nL	=	Displacement in steps of length
k_n	=	Normal stiffness
k_s	=	Shear stiffness
L_s	=	Joint length
N	=	Number of smaller objects
r	=	Rebound number
R	=	Size of smaller object
S	=	Shear intercept
SF	=	Structural function which is mean square of first order derivative of profile
T	=	Transmissivity of fractured rock
u_n	=	Normal deformation
u_s	=	Shear deformation
W	=	Weight of upper block
Z_2	=	Root mean square of first order derivative of profile.
β_s	=	Angle of inclination
γ	=	Density of rock
γ_e	=	Effective specific weight of rock mass

φ_μ	=	Frictional angle
ρ	=	Density of fluid
σ_n	=	Normal stress
τ	=	Shear stress
μ	=	Fluid viscosity

.

Chapter- 1

INTRODUCTION

1.1 INTRODUCTION

Joints, discontinuities of geological origin such as fault, fold, bedding and fractures exists within almost all rock masses and often govern the strength of discontinuous masses. These joints and discontinuities change engineering behavior of rocks tremendously when compared with that of intact masses. Generally deformations in discontinuous rock masses are comparatively more than intact rock masses under same stress condition. Study of rock joints, is crucial to the development of infrastructure and mining projects. As, joints control the:

- design and construction of cut slopes for roads, railways and open cut mines;
- stability of rock abutments for dams;
- rock extraction strategies in underground mines;
- stability of natural rock slopes and the assessment of landslip potential;
- design of foundations for large structures on rock;
- viability of long-term waste storage solutions;
- design of support and lining solutions for tunnels and underground openings.

From the above wide-ranging list, it is obvious that rock joints have a significant influence on the activities of our community [9].

To consider the effect of joints and discontinuities on deformability of rock masses, the deformability of rock discontinuities should be known first. The deformation properties of individual rock discontinuities can be described by their stiffness characteristics i.e. normal stiffness and shear stiffness. Most of civil engineering activities in rocks are mainly concern with low confining pressures or uniaxial compression condition. For safe and efficient design of any structure in rock mass, it is crucial to assess the deformational characteristics of the rock mass to reasonable accuracy under these conditions.

Since beginning of studies on rock mechanics and geotechnical engineering various researchers have studied the behavior of failure in discontinuous rock masses, *Bandis et el.* (1983) studied behaviour of rock joint deformation and gave non linear relation depending on type of joint [1].

The deformation properties of rock joints can be described by stiffness characteristics. These characteristics are namely shear stiffness and normal stiffness. Shear stiffness of a rock joint can be estimated by conducting the direct shear test and the normal stiffness can be evaluated from the direct compression test. These stiffness characteristics are required to understand deformation in practice and also the same is required as an input by professional software for various analysis and design.

1.2 OBJECTIVE

The aim of current work is to determine the stiffness characteristics of rock for two different types of roughness profiles under different stress conditions. The two types of joint surfaces are

Type I : Naturally broken joint
Type II: Hacksaw tooth cut joint

For determining shear stiffness, the direct shear apparatus has been used for both type of joints and for determining normal stiffness, the compression strength test equipment has been used. Number of joints has been varied from 1 to 4, to find the normal stiffness for both types of joints. Model material simulating the soft rock joint has been selected for the tests. The model material used in the study is Plaster of Paris. Plaster of Paris specimens has been prepared in laboratory and was tested in different conditions.

1.3 ORGANIZATION OF THE THESIS

- Chapter 1 introduces and briefly describes the objective and scope of present study.
- Chapter 2 consists of critical review of literature concerning the significance of various joint roughness properties and the deformational properties.
- Chapter 3 gives the detailed experimental program and description of experimental set up to predict the stiffness characteristics of joints.
- Chapter 4 deals with the presentation of the experimental results and the estimated stiffness characteristics.
- Chapter 5 includes major conclusions of the work.

CHAPTER 2
LITERATURE REVIEW

2.1 INTRODUCTION

Rock masses are far from being continua and consist essentially of two constituents: intact rock and discontinuities (planes of weakness). The existence of one or several sets of discontinuities in a rock mass creates anisotropy in its response to loading and unloading. Also, compared to intact rock, jointed rock shows a higher permeability, reduced shear strength along the planes of discontinuity and increased deformability and negligible tensile strength in directions normal to those planes. Furthermore, discontinuities create scale effects. Finally, discontinuities form blocks by intersection that can result in stability problems during surface or underground excavations.

With few exceptions, it is incorrect to ignore the presence of discontinuities when modeling rock mass response to loading and unloading. Strength and deformations are two important design parameters, which need to be estimated reliably while studying jointed rocks. The study of properties of rock mass is the determination of the characteristics of joints. According to *ISRM* (1978), rock mass can be classified by different parameters like orientation, roughness, wall strength, aperture, seepage and number of joints sets and block size. Among these properties the most important factors affecting strength and deformation are the roughness, frequency and orientation of joints. The various significant rock properties are discussed in current chapter.

2.2 PROPERTIES OF ROCK JOINTS

2.2.1 Roughness of Joints

In almost all real situations joints in rock are non planar and are inclined as shown in Fig 2.1. Here inclination of asperity is 'i' and angle of friction is φ_μ. At the moment of peak shear stress, the resultant force on the joint, R, is then oriented at an angle φ_μ with the normal to the surface on which motion is about occur, since the surface is inclined i

degrees with the joint plane, the joint friction angle is φ_μ + i when referred to the direction of mean joint plane. The accuracy of this simple concept was demonstrated by *Patton* (1966) [8].

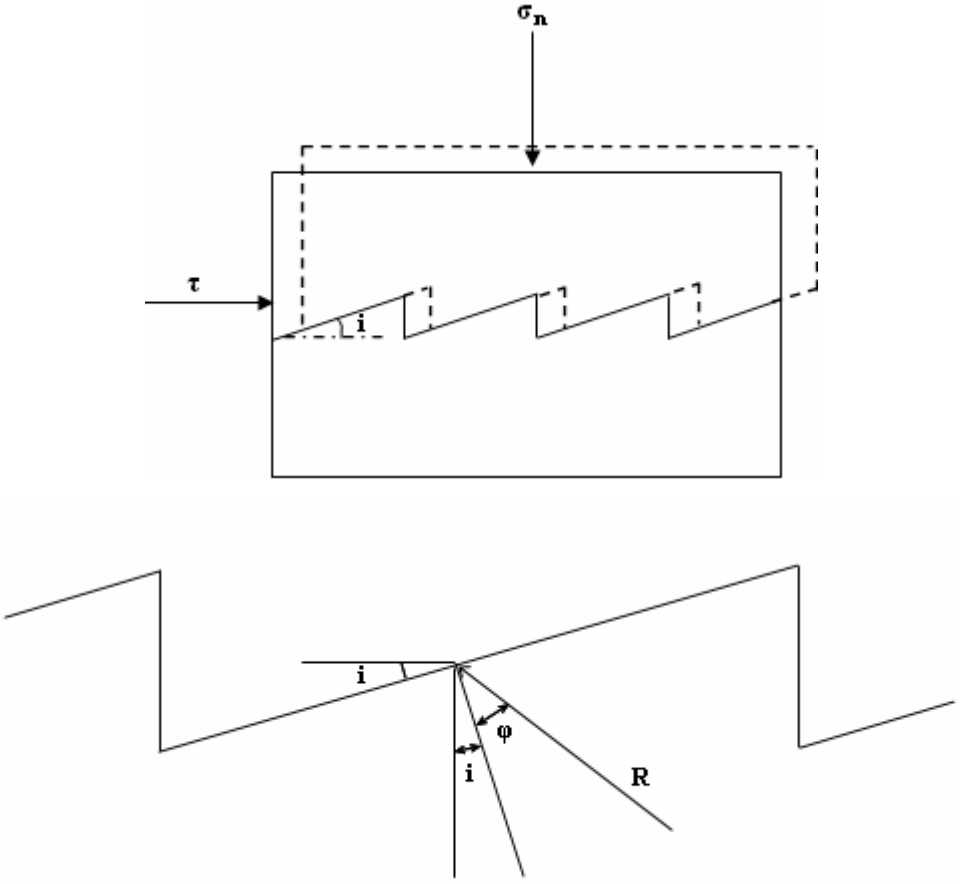

Fig 2.1 The Basis For Patton's Law for Joint Shear Strength [8].

If the normal pressure is relatively large, it will be easier to shear the joint through the teeth along its surface than to lift over them. Mobilizing some rock strength by failure through the teeth generates a shear strength intercept *S* and a new frictional angle φ_μ related to sliding on surfaces broken through the rock and thus approximated by the residual frictional angle for intact rock specimens. The residual friction angle is the slope of the linear envelope to a series of Mohr circles through residual stress values for a series of triaxial compression tests with intact rock specimens. Fig 2.2 shows the bilinear failure criterion for joints representing the merging of Patton's law and the condition for shearing through asperities.

$$\tau = \sigma_n \tan(\varphi_\mu + i) \quad \text{for smaller } \sigma_n \qquad (2.1)$$

$$\tau = S + \sigma_n \tan(\varphi_\mu) \quad \text{for larger } \sigma_n \qquad (2.2)$$

Where,

τ	=	shear strength along joint
σ_n	=	Normal stress on plane of sliding
φ_μ	=	frictional angle along joint
i	=	roughness angle or angle of asperity
S	=	cohesion intercept

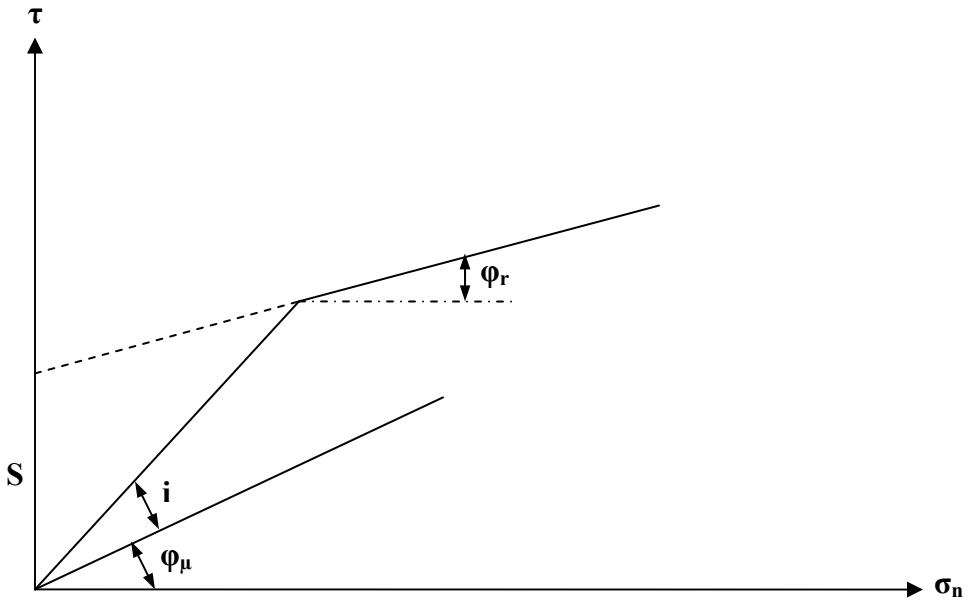

Fig 2.2 Bilinear Shear Strength Criteria. [8]

Theories of joint strength effecting this transition smoothly were presented by *Ladanyi* et. al. (1970), *Jaeger* (1971) and *Barton* (1973) and were reviewed by *Goodman* (1976) [8]. The value of φ_μ by many investigators was found to be around 40°. This value for variety of rocks with saw cut or ground surface up to normal stress 200 MPa.

Barton and Choubey (1977) gave a relationship between joint roughness and joint shear strength by conducting direct shear test on tension fractures produced in rocks of different strengths [6]. The equation given was

$$\frac{\tau}{\sigma_n} = \tan\left((90 - \varphi_\mu)\frac{d_n}{\varphi_\mu} + \varphi_\mu \right) \qquad (2.3)$$

Where,

τ	=	shear strength of joint
σ_n	=	normal stress
φ_μ	=	frictional angle
d_n	=	peak dilation angle

2.2.2 Joint Roughness Coefficient

Barton (1976) observed that rock joints exhibit a wide range of shear strength due to variable surface roughness and rock strength. He proposed following empirical relation to predict shear strength [4]. The given equation follows nonlinear law of friction.

$$\tau = \sigma_n \tan\left(JRC \log\frac{JCS}{\sigma_n} + \varphi_\mu \right) \qquad (2.4)$$

Where,

τ	=	peak shear strength of joint
σ_n	=	effective normal stress
JRC	=	joint roughness coefficient
JCS	=	joint wall compressive strength
φ_μ	=	angle of friction, which ranges from 25° to 35° for most rock joint surfaces.

The joint wall compressive strength (JCS) is equal to unconfined compressive strength of rock for an unweathered joint and is equal to ¼ of unconfined compressive strength if origin of joint is due to weathering. This value for many rocks lies in the range of 0.1 to 2 MPa.

Barton and *Choubey* (1977) suggested that this value can be estimated in field or laboratory using a Schmidt Hammer test [6]. The joint roughness coefficient represents a sliding scale of roughness which ranges from 0 to 20 for roughest to smoothest surface.

By performing shear test the value of JRC can be calculated as,

$$JRC = \left(\frac{\arctan \frac{\tau}{\sigma_n} - \varphi_b}{\log \frac{JCS}{\sigma_n}} \right) \qquad (2.5)$$

Tse and *Cruden* (1979) studied the roughness profiles presented by Barton on classifying different joint roughness coefficient [22]. They presented the following equation.

$$JRC = 32.2 + 32.47 \log Z_2 \qquad (2.6)$$

$$JRC = 32.8 + 16.58 \log SF \qquad (2.7)$$

Where,

Z_2 is root mean square of first order derivative of profile.

SF is structural function which is mean square of first order derivative of profile.

Mandelbrot (1977) gave the concept of fractals to describe the relations of irregularly shaped objects which exhibits similar property [10]. According to fractal geometry, profiles of joint surface can be measured by a number termed fractal dimension (D). This value lies between 1 to 2. If a fractal object is divided into N numbers of smaller objects each with a size R, then:

$$D = \frac{\log N}{\log \frac{1}{R}} \qquad (2.8)$$

Assuming the rock surface profiles are self-similar fractals, Cart and Warriner, Lee et al., and Wakabayashi and Fukushige have developed relationships between D and *JRC* [10]*:*

Carr and *Warriner* (1989)

JRC = -1022.55 + 1023.92D (2.9)

Lee et al., (1990)

$$JRC = -0.878 + 37.7844\ (D - 1)/0.015 - 16.9304\ [D- 1)/0.015]^2 \quad (2.10)$$

Wakabayashi and *Fukushige* (1992)

$$JRC = SQRT\ [(D - 1)/0.00004413] \quad (2.11)$$

Turk et al. (1987)

$$JRC=-1138.6 + 1141.6D \quad (2.12)$$

Eq. (2.12) was developed by the authors of this paper by linear regression of the data given by *Turk et al.* (1987) with the coefficient of determination equal to 0.84. *Carr and Warfiner* (1989) developed Eq. (2.9) using the data collected from a joint face of size 150 x 15 m at Libby Dam, Montana. The spacing between two consecutive measurement points was 15.2 cm. *JRC* values were estimated by matching with the standard profiles. *Lee et al.* (1990) *and Wakabayashi and Fukushige* (1992) developed the relationships by digitizing the ten standard profiles. Although it was not mentioned specifically, the interval used by *Lee et al.* was about 0.5 mm and the divider lengths used were 1, 2, 3, and 5 mm. Divider lengths 0.05 to 5 mm were used by *Wakabayashi and Fukushige*. *Turk et al*, used divider lengths of 2, 6, 20, 60 mm.

In general JRC can be assessed by profiling methods. One of these profiling methods is to use the carpenters comb. In this three profiles of a joint can be taken one along center and others on either side. The profiles are traced on to a paper and digitized to determine the profile conditions. Then the data representing the digitized profile is run through a computer program to obtain JRC value.

2.2.3 Orientation of Joints

The affect of the orientation of joint system with respect to stress is a complex problem. Therefore to simplify, effect of single plane of weakness has been considered on strength

of joint. Generally, Mohr Coulomb's equation is adopted as the criteria for slip in single plane. [8]

$$\tau = c + \sigma_n \tan\varphi \qquad (2.13)$$

Where,

τ	=	Shear stress
c	=	Cohession
σ_n	=	Normal stress
φ	=	Angle of internal friction.

2.2.4 Dilation

Dilation is the property which enables the expansion of rock joints. Or in other words it is the relative movement between two jointed faces along profiles.

Barton and Choubey (1977) studied dilation in rock and concluded that surfaces having high joint compressive strength and high joint roughness coefficient will dilate strongly at the instant of peak strength [6]. They observed maximum dilation angle occurs more or less simultaneously with peak shear strength, called as peak dilation angle (d_n). The majority of d_n values lies between the limits $0.5JRC\log_{10}\left(\frac{JCS}{\sigma_n}\right) < d_n < 2JRC\log_{10}\left(\frac{JCS}{\sigma_n}\right)$ and mean value of initial dilation angle, d_i for 136 specimen was 6.6°, roughly 1/3 of d_n. Both d_n and d_i can be zero occasionally. However, their study was confined in peak dilation angle and initial dilation angle.

Fecker and Renger (1971), also studied dilation in jointed rock [18]. They concluded that all the asperities are overridden and there is no shearing of, dilation for any displacement *nL* depends on tan d_n given by following relation.

$$h_n = nL \tan d_n \qquad (2.14)$$

where,

h_n	=	Dilation
nL	=	Displacement in steps of length

d_n = Maximum angle between the reference plane and profile for the base length.

Dilation can also be represented by dilation angle d = V/H, where V is the vertical displacement in direction perpendicular to shear force and H is the horizontal displacement in the direction parallel to applied shear force.

2.2.5 Scale Effects

Barton and Choubey (1977) noted significant scale effects in relation to JRC and JCS. As the joint length increases, joint wall contact is transferred to the larger and less steeply inclined asperities as the peak shear strength is approached, resulting in larger individual contact areas with correspondingly lower JCS values [6]. The larger contact areas will also be less steeply inclined in relation to the mean plane of the joint when compared to the small, steep asperities, resulting in reduced JRC values. Consequently, the reduction in JRC and JCS values will result in a reduction in shear strength as the discontinuity length is increased.

Barton and Bandis (1982) observed scale effects during the direct shear test [23]. Following correction factors were suggested after undertaking extensive joint and joint replica testing and a literature review for joint length L.

$$JRC_n \approx JRC_o \left(\frac{L_n}{L_o} \right)^{-0.02 JRC_o} \qquad (2.15)$$

$$JCS_n \approx JCS_o \left(\frac{L_n}{L_o} \right)^{-0.02 JRC_o} \qquad (2.16)$$

Where, the subscripts ‘‘0’’ and ‘‘n’’ refer to laboratory scale (100 mm) and in situ block sizes, respectively.

Yashinaka and Yambe (1986) have presented the shear strength of rock mass as a function of area to consider the scale effect [24]. The relation was given by

$$\tau_p = k(\sigma_n)^{\alpha} A^{\beta} \qquad (2.17)$$

Where, α, β, k are the constants and A is the area of joint.

Pratt et al. (1972) reported scale effects on compressive strength test by conducting a series of unconfined compression tests on specimens of quartz and diorite ranging in length from 5 cm to 275 cm [19]. They found that compressive strength dropped from about 60% to 70% for 5 cm long specimens, down to about 7 MPa for 90 cm long specimens. Beyond length of 100cm, the scale effect is not appreciable. Subsequently *Pratt et al.* (1974) investigated scale effects on the shear strength of joints in quartz diorite over a range of 60 m^2 to 5000 m^2 surface area, and found that shear strength dropped by about 40% [19].

2.2.6 Joint Intensity

The intensity of joint is the number of joints per unit distance normal to the plane of the joints in a set. It also influences the strength and deformation behaviour of rocks. This is concluded by many investigators after carrying out model studies. Since it is very difficult to ascertain the behaviour of jointed rock mass in the field, therefore model depicting joints of many configurations simulating joints of rock mass were prepared and tested by different investigators, under different stress conditions.

2.3 ESTIMATION OF JRC AND JCS

Surface roughness plays an important role in determination of strength and deformation properties of jointed rock. This section deals with a various methods and tests suggested by researchers to estimate roughness by determining JRC and JCS.

An approach to the problem of predicting the shear strength of rough discontinuities was proposed by *Barton* (1975) [3]. Based upon careful tests and observations carried out on an artificially-produced rough joint in material used for model studies, Barton developed the 10 typical profiles of increasing roughness and assigned coefficients ranging from 0 to 20 forming 10 joint roughness coefficient (JRC) ranges as shown in Fig.2.3. These standard profiles were later adopted by the International Society for Rock Mechanics in their suggested procedure for measuring the roughness of discontinuities.

They also described a residual tilt test in which pairs of flat sawn surfaces are mated and the pairs of blocks are tilted until sliding occurs. If as is the tilt angle at which sliding starts to occur, σ_n is the normal stress acting on the joint when sliding begins to occur and φr is the residual friction angle, the JRC value can be estimated from the following equation:

$$JRC = \frac{\alpha - \varphi_r}{\log\left(\frac{JCS}{\sigma_n}\right)} \qquad (2.18)$$

The normal stress (σ_n) is calculated using

$$\sigma_n = \frac{W \cos \beta_s}{A} \qquad (2.19)$$

where W is the weight of the upper block, A is the gross contact area, and β_s is the inclination angle.

Among Other estimation method, *Barton* and *Bandis* (1990) presented a method for estimating JRC from the J_r component of the Q rock mass classification system [23].

Where the state of weathering of both the rock material and the joint walls is similar, samples of rock material tested in uniaxial compression can be used to estimate JCS. Where joint walls are weathered to a limited depth, methods of point load testing (*Hoek et al.*1981) and Schmidt hammer (*Muller*, 1965) techniques may be appropriate. Where no direct measurements are available, a ratio of JCS/σ_c equal to 1/4 may be used (*Barton*, 1973) or field index testing may be used [23].

The Schmidt's hammer test provides an ideal solution to determine the JCS. It is a simple device to record the rebound of a spring load plunger after its impact on the surface. It is suitable for measuring JCS values from 20 MPa to 300 Mpa. *Muller* gave a wide range of Schmidt's Hammer tests for use in Rock Mechanics to estimate JCS. *Barton* and *Choubey* (1977) gave following relation to calculate JCS [23].

$$\log(JCS) = 0.00088\gamma r + 1.01 \qquad (2.20)$$

Where, γ is the density of rock and r are the rebound numbers from Schmidt's Hammer test on rock joint wall.

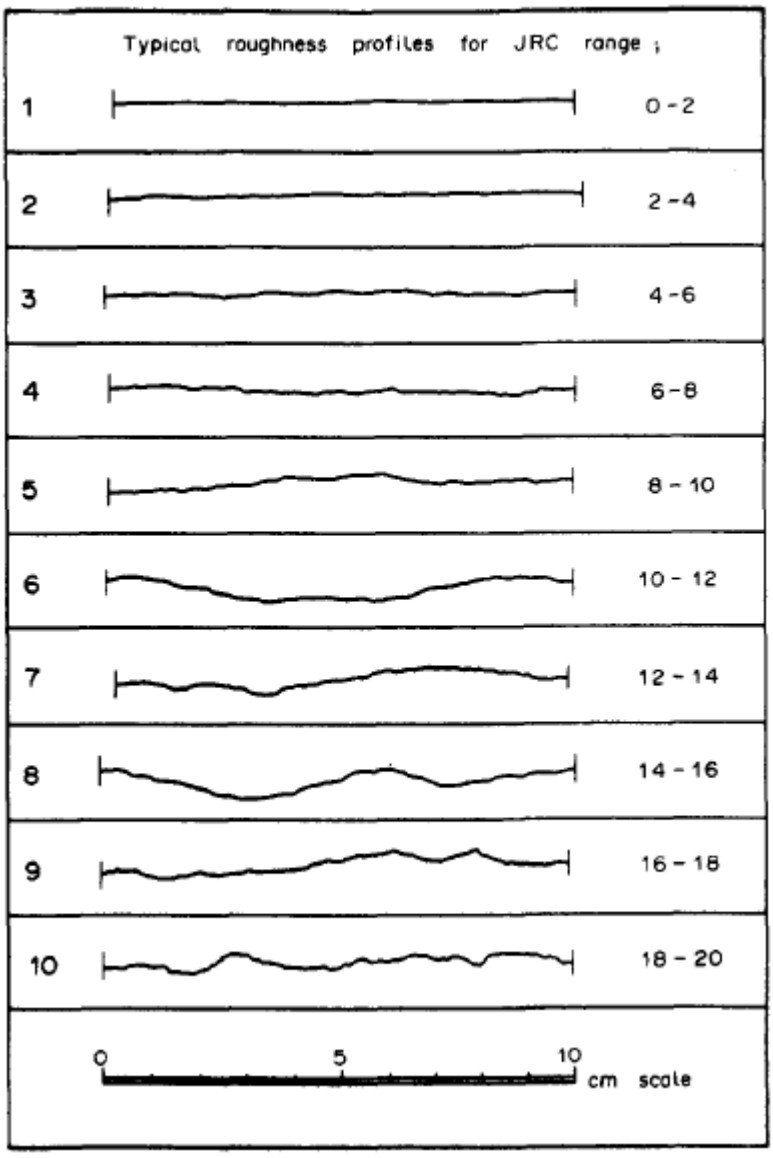

Fig 2.3 Roughness Profiles and Corresponding Range of JRC Values [17]

2.4 DEFORMATIONAL BEHAVIOUR OF JOINTED ROCK

Joint deformation is a fundamental component of the performance of a discontinuous rock mass under changing stress conditions. At the relatively low stress levels encountered in near-surface excavations, the deformation of joints dominates the elastic deflection of the intact rock. Even under the higher levels of stress associated with heavy structures, the slippage and closure of joints constitute the major part of settlement on rock.

It is well known that the deformation behaviour of a jointed rock mass is greatly influenced by the deformability of joints; and the deformation moduli of rock masses decreases remarkably in comparison with those of intact rock when joints are present. Therefore, *in situ* testing such as plate loading and radial jacking have been generally performed in practice for determining the rock mass moduli values. However, the deformation characteristics of a rock mass depend on the orientation of joints with respect to the loading direction, the *in situ* stress condition (confining stress) and the relative size between the spacing of joints and the size of the loaded region. It is very difficult to evaluate the deformability of a rock mass that correctly corresponds with the general conditions mentioned above.

Seidel and Haberfield (2002) state that the shear behaviour of joints with more complex geometry is also controlled by two basic and independent mechanisms i.e initial sliding along the surface of asperities and simultaneous shearing through all of the intact asperities [20]. The mechanisms cannot be readily isolated in the joint response. Shear displacement is initially affected by sliding on the steepest asperities. The consequence of this sliding is joint dilation, which causes shallow asperities to be lifted out of contact, and stresses to be localized on the steep asperities in contact. At a critical displacement, the shear stresses on the steepest asperity exceed the asperity strength. The asperity fails, and its load is shed to other asperities. Dilation is then controlled by the next steepest asperity until it too fails in shear. Thus, sliding, progressive asperity shear and post-peak sliding occur simultaneously in complex profiles.

Joint deformability can be described by the character of the stress-deformation curves. *Goodman et al.* (1970) introduced the terms "normal stiffness" (k_n) and "shear stiffness" (k_s) to describe the rate of change of normal stress (σ_n) with respect to normal displacements (u_n) and of the shear stress (τ) with respect to shear displacements (u_s) respectively [8].

2.4.1 Normal Stiffness

When a compressive normal stress (σ_n) is applied on jointed rock it shows some deformation (u_n). This deformation is mainly due to closing of joints in rock. A curve can be plotted between normal deformation and normal stress. Slope of tangent drawn at any point on this curve gives the normal stiffness of the joint at that point. Mathematically it can be defined as

$$k_n = \frac{\Delta\sigma_n}{\Delta u_n} \qquad (2.21)$$

Here Δ denotes an increment.

Barton (1972) describes joint normal stiffness (k_n) as the normal stress per unit closure of the joint. *Bandis et al*. (1983) proposed that joint normal stiffness is influenced by

- the initial actual contact area;
- the joint wall roughness;
- the strength and deformability of the asperities; and
- the thickness, type and physical properties of any infill material [23].

Joint normal stiffness can be estimated from laboratory testing. The UDEC user's manual (1996) states that the normal stiffness for rock joints with clay-infilling can range from roughly 10 to 100GPa/m while that for tight joints in granite and basalt can exceed 100 GPa/m. *Coulthard* (1999) presents typical ranges for joint normal stiffness including values of 300–550 GPa/m for basalt.[23]

Jiang et al. (2009) developed a new method for determination of normal stiffness of fractured rocks by combing hydro and mechanical properties, relationship between

transmissivity and depth is utilized to calculate normal stiffness of large-scale fractured rock masses [16]. The basic idea is that flow in fractured media is very sensitive to aperture of discontinuity, and the aperture of the discontinuity is mainly determined by the normal stress and normal stiffness. A decrease in transmissivity of fractured rock masses with increasing depth, as indicated in hydraulic tests, is due to closure of the joints caused by an increase in the normal stress that is nearly proportional to depth. Consequently, it is possible to estimate in-situ fracture normal stiffness by using information of depth-dependent transmissivity. They derived an equation as,

$$k_n = -\frac{3\gamma_e}{\left(\frac{12\mu f}{\rho g}\right)^{\frac{1}{3}}} \times \frac{T^{\frac{2}{3}}}{\frac{dT}{dh}} \qquad (2.22)$$

Where,

γ_e is the effective specific weight of rock mass.

T is the transmissivity of fractured rock.

μ is fluid viscosity.

f is friction factor accounting for roughness of joint surface.

ρ is density of fluid.

g is acceleration due to gravity.

h is the depth.

2.4.2 Shear Stiffness

A jointed rock goes under shear deformation (u_s) on applying shear stress (τ). A curve can be plotted between shear deformation and shear stress. Slope of tangent drawn at any point on this curve gives the shear stiffness of the joint at that point. It can be given as

$$k_s = \frac{\Delta\tau}{\Delta u_s} \qquad (2.23)$$

Here Δ denotes an increment.

The shear stress and deformation values are influenced by the applied normal stress. The shear behaviour of planar rock joints can be investigated in the laboratory by using a conventional direct shear apparatus where the normal load is kept constant during the shearing process. However, for non planar discontinuities, shearing results in dilation as one asperity overrides another, and if the surrounding rock mass is unable to deform sufficiently, then an inevitable increase in the normal stress occurs during shearing. (*Indraratna and Hauqe,* 1997 [12])

Barton (1972) described joint shear stiffness (Ks) as the average gradient of the shear stress-shear displacement curve for the section of the curve below peak strength. Shear stiffness can be estimated from direct shear testing results, and its value will depend on the size of a sample tested and will generally increase with an increase in normal stress (*Bandis et al*, 1983). *Barton* and *Choubey* (1977) suggested the following equation for the estimation of the peak shear stiffness (MPa/mm) [23]:

$$k_s = \frac{100}{L_x}\sigma_n \tan\left[JRC \log_{10}\left(\frac{JCS}{\sigma_n}\right) + \varphi_r \right] \qquad (2.24)$$

where L_x is the joint length in metres. Use of the equation requires the assumption that the peak shear strength is reached after the shearing of approximately 1% of the joint length. If the scale effect does not die out within the critical discontinuity length (L_{crit}), the value of Lx should not exceed L_{crit} [23].

The UDEC user's manual (1996) states that the shear stiffness for rock joints with clay-infilling can range from roughly 10–100 MPa/m while that for tight joints in granite and basalt can exceed 100 GPa/m. Coulthard (1999) presents typical ranges for joint shear stiffness including values of 250–450 GPa/m for jointing in basalt. [23]
Many researchers have done the experiments and estimated the stiffness values for different materials. Those values are tabulated in Table 2.1

Table 2.1 Joint Stiffness Values of Model Materials [18]

Material Description	Shear Stiffness (MPa/mm)	Normal Stiffness (MPa/mm)	UCS (MPa)	Reference
Plaster of Paris	0.21-0.52	2.5-24	7.61	Kulatialake et al (2001)
Lime Silica	0.586 (avg)	23.5-42.8	17.13	Singh (2000)
Sand + Plaster of Paris	0.31-0.41	8.0-16.0	-	Huang et al (1995)
Cement + Sand Mortar	0.225 (max)	19.8-52	23.6	Kumar(2000)
Sand Lime	0.14-0.35	11.2-68	13.5	Tiwari (2005)

CHAPTER 3
EXPERIMENTATION

The Chapter describes the experimental investigation carried out in Laboratory in order to predict the stiffness characteristics of rock joints using direct shear test and compressive strength test equipments. The objective of the study can be described as follows.

- Conducting the test on laboratory prepared Plaster of Paris specimens by using aforesaid equipments
- Conducting the tests under different normal stresses as well as different roughness profiles for specimens with varying number of joints.

3.1 MATERIAL USED

Model material simulating the soft rock joint has been selected conforming Deere and Millers (1966) classification (Table 3.1 & Fig. 3.1). In the present study, average value of UCS of Plaster of Paris came out to be 5.43 MPa and average Young's Modulus came out to be 922 MPa. According to *Deere* and *Miller* Classification (1966) these values fall under EL group which classifies as soft rock. Also from ISRM (1979) shown in Table 3.2 declares the rock to be in low strength if UCS is in the range of 2-25 MPa. From here we can consider Plaster of Paris as soft rock.

Table 3.1 Deere and Miller Classification of Rocks [7]

Description	Unconfined Compressive Strength (MPa)
Very High Strength	Above 224
High Strength	113 – 224
Medium Strength	56 – 112
Low Strength	28 – 56
Very Low Strength	Below 28

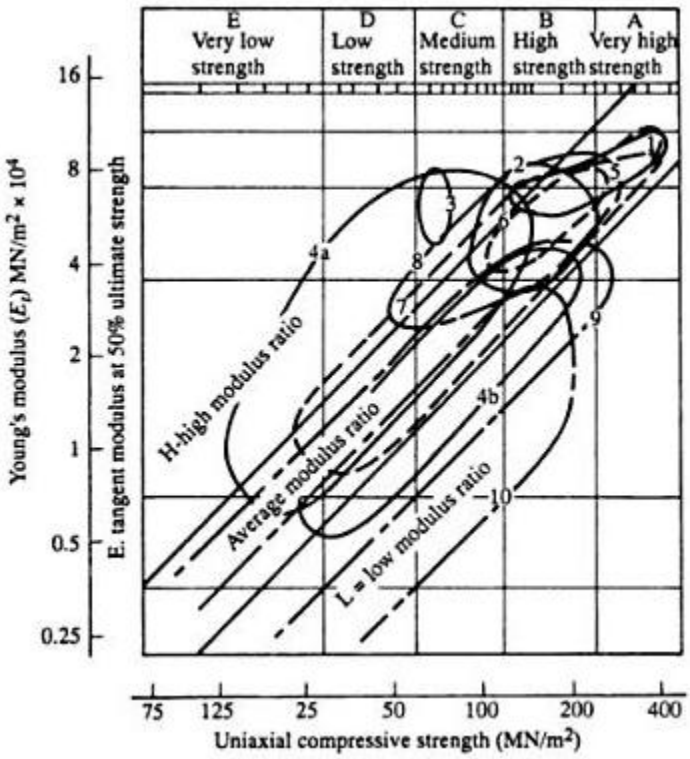

Fig. 3.1 Engineering Classification of Intact Rock after Deere & Miller (1966) [7]

Table 3.2 Strength classification of intact rock [21]

Description	Unconfined Compressive Strength (MPa)
Very High Strength	250 – 700
High Strength	100 – 250
Medium Strength	50 – 100
Moderate	25 – 50
Low Strength	2 – 25
Very Low Strength	1 – 5

Plaster of Paris is used for preparing the testing specimens because it can be used to make idealized soft rock joints, mainly because this material is universally available and is inexpensive. It can be moulded into any shape when mixed with water, and long term strength is independent of time once chemical hydration is completed. Plaster of Paris is

prepared from gypsum (Calcium sulphate dihydrate, $CaSO_4.2H_2O$). When gypsum is heated to 120°C it loses 75% of its water of crystallization to form plaster of Paris. [12]

$$2(CaSO_4.2H_2O) \xrightarrow[120^0 c]{} (CaSO_4)_2.H_2O + 3H_2O \quad (3.1)$$

When this white powder is mixed with water, it forms a plastic mass.

$$(CaSO_4)_2.H_2O + 3H_2O \xrightarrow[120^0 c]{} 2(CaSO_4)_2.2H_2O \quad (3.2)$$

The Plaster of Paris for experimentation was observed having initial setting time of 10-12 min and final setting time of 20-23 min when mixed with water in ratio of 5:3 by weight. After final setting this mass sets into a hard solid mass constituting interlaced gypsum crystals.

The basic properties of the model material were determined by performing many tests on cube of size 70mm. Specimens after a curing period of 14 days at room temperature, the air cured plaster showed a consistent average unconfined compressive strength of 5.43 MPa and an average Young's Modulus of 922 MPa.

3.2 SPECIMEN PREPERATION

Specimens were prepared by adding 60 % water by weight to the plaster of Paris and air curing them for 14 days. The size of specimens were governed by the size of shear box in the shear testing apparatus having cross sectional area of 60mm x 60mm. The two types of joints were formed as

- **Naturally broken joint:** By creating a fracture plane with hacksaw on all four sides of specimens and then chiseling at the fracture plane. (Fig3.2)
- **Hacksaw tooth cut joint:** By cutting the specimens in height from middle using Hacksaw blade. (Fig 3.3)

`Specimens with both these joint surfaces were also prepared having

- One joint,
- Two joints,
- Three joints and,
- Four joints.

3.3 PROCEDURE FOR DIRECT SHEAR TEST

IS 2720 (PART XIII) gives detail of Direct Shear Test. HS 24.15 Direct Shear Apparatus (Electronic unit) which follows IS 2720 (PART XIII) has been used in present work. This has a maximum normal load capacity of 0.8MPa. The shear box apparatus as shown in Fig. 3.6 is made into two halves. The top half slides over the lower half at a constant rate by geared jack, driven by electric motor and is fitted with a loading U-arm that has been connected to proving ring. The upper half of the specimen is held in the upper box and the lower half in the lower box, and the joint between the two parts of the box is at the level of joint of specimen. Normal load is applied to the specimen through the lever arm and from the loading yoke bearing upon steel ball of pressure pad. When a shearing force is applied to the lower box through the geared jack, the movement of the lower part of the box is transmitted through the specimen to the upper part of the box and hence on the load cell (maximum capacity of 2250N). This load indicates shear force. The displacement during the shearing process is measured by strain gauge. The complete setup is as shown in Fig 3.7

The specimen in the shear box is sheared under a normal load. The test is conducted till failure. A graph is plotted between the shear stress and the deformation. The slope of the tangent at any point on the curve is known as the shear stiffness of the joint.

In the present work, the tests were conducted on specimen of cross sectional size 60mm x 60mm for both Natural and hacksaw type of joints under the normal stress levels of 0.1, 0.25 and 0.5 MPa.

Fig 3.2 Preparation of Type I Joint Surface

Fig 3.3 View of Type I Joint Surface

Fig 3.4 Preparation of Type II Joint Surface

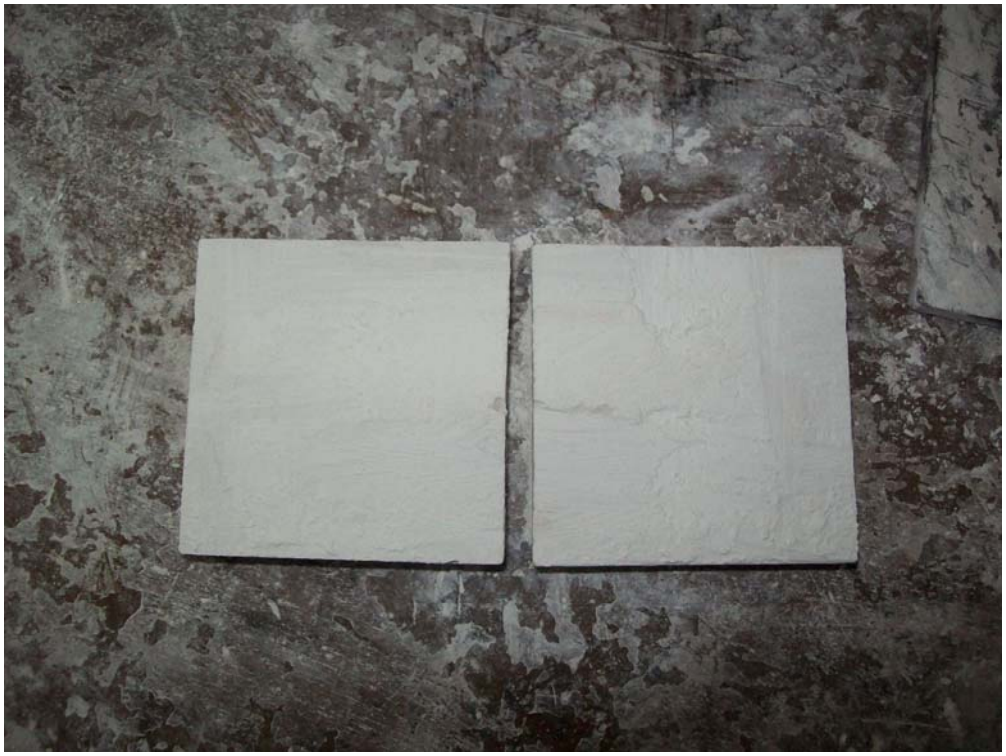

Fig 3.5 View of Type II Joint Surface

Fig 3.6 Shear Box Apparatus

Fig 3.7 Direct shear Testing Equipment

Fig. 3.8 Compressive Strength Testing Equipment

3.4 PROCEDURE FOR COMPRESSIVE STRENGTH TEST

Specimens of cross sectional area of 60mm x 60mm with one, two, three and four joints having both Natural and Hacksaw discontinuities were tested. A general arrangement has been shown in Fig. 3.8.

The specimen is placed between two plates and a proving ring to measure load has been placed above it. A dial gauge was fitted on the lower plate to determine deformation. Lower plate moves up at a constant rate with the help of electric motor, applying load on the specimen. The Normal load in the proving ring was noted with respect to the deformation in the dial gauge up to the failure. A curve is plotted between Normal stress and deformation. The slope of the tangent at any point gives the Normal Stiffness of the joint.

CHAPTER 4
RESULT & DISCUSSION

In this chapter, the experimental results of the direct shear test and compressive strength test on laboratory prepared specimens have been presented. The peak shear stress variation with respect to normal stress has been reported. Over and above, shear stress vs deformation plots were made to study the variation of two types of joints at each normal stress level i.e at 0.1, 0.25 and 0.5 MPa. An empirical equation has been derived to show the correlation between shear stiffness and normal stress. Hence, shear stiffness can be estimated once the normal applied stress is known.

4.1 STIFFNESS CHARACTERISTICS

The direct shear test and compressive strength test were conducted on two types of joints and results are discussed below.

4.1.1 Shear Stiffness

1. **Type I Joint-** The direct shear tests were conducted and obtained curves are shown in Fig.4.1 to 4.9. The shear stiffness values are calculated for deformation corresponding to peak shear stress values after considering corrected area as per IS 2720 (PART XIII). The results have been summarized in table 4.1. Peak shear stresses values increases with increase in applied normal stress. Moreover, the variation of shear stresses was non linear against deformation. Peak shear stresses values ranges from 0.116 – 0.152, 0.274 - 0.293 and 0.483 - 0.586 for normal stress values of 0.1, 0.25 and 0.5 MPa. The shear stiffness lies in a range from 0.023 to 0.143 MPa/mm.

2. **Type II Joint-** The direct shear tests were conducted and obtained curves are shown in Fig.4.10 to 4.18. The shear stiffness values are calculated for deformation corresponding to peak shear stress values after considering corrected area as per IS 2720 (PART XIII). The results have been summarized in Table 4.2.

Peak shear stresses values increases with increase in applied normal stress. Moreover, the variation of shear stresses was non linear against deformation. Shear stiffness ranges from 0.125 – 0.159, 0.216 - 0.325 and 0.461 - 0.549 for normal stress values of 0.1, 0.25 and 0.5 MPa. The shear stiffness lies in a range from 0.037 to 0.129 MPa/mm.

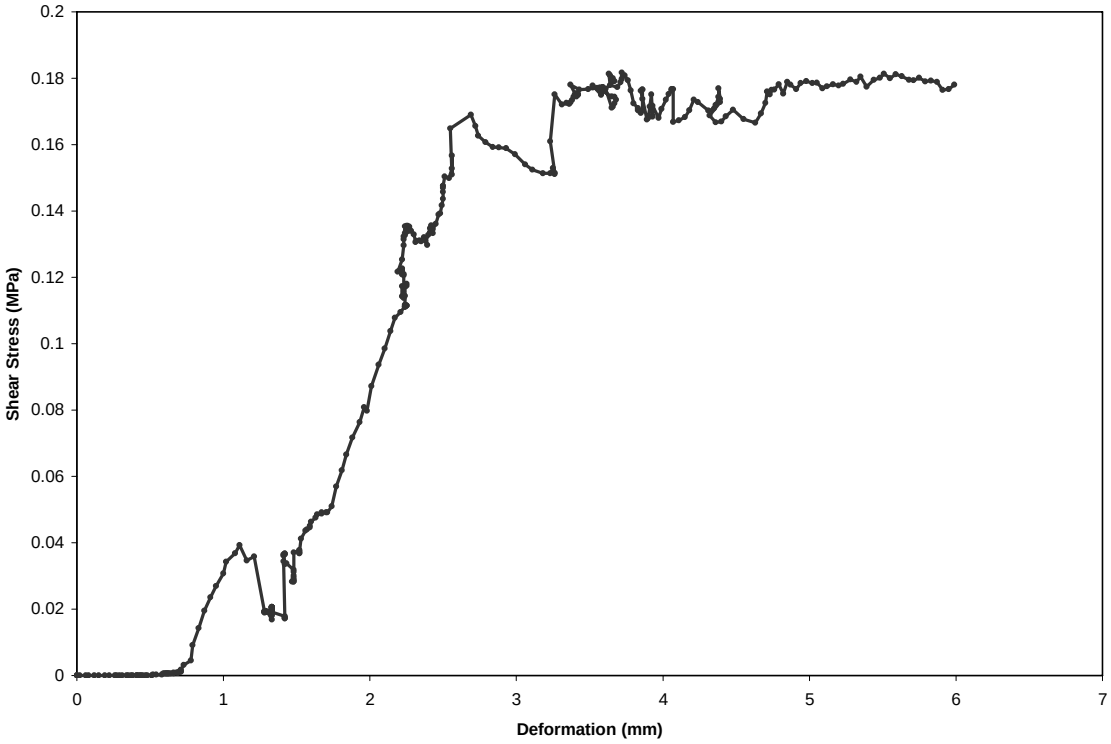

Fig 4.1 Deformation Vs Shear Stress for Type I Joint at 0.1 MPa Normal Stress for Sample A

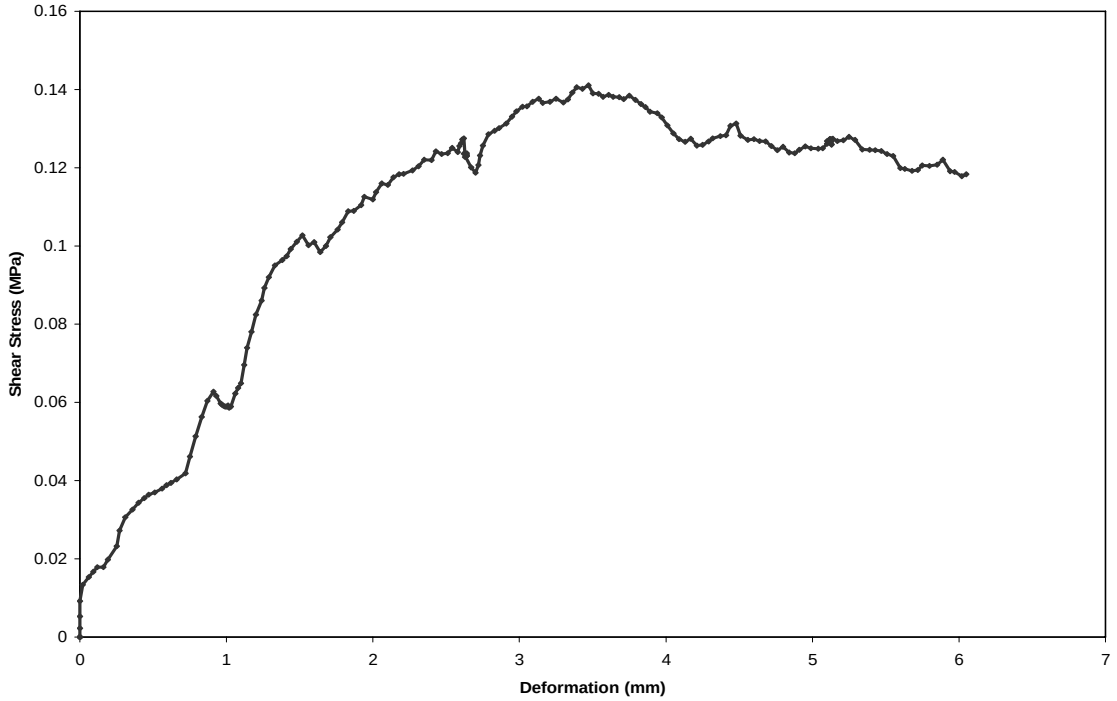

Fig 4.2 Deformation Vs Shear Stress for Type I Joint at 0.1 MPa Normal Stress for Sample B

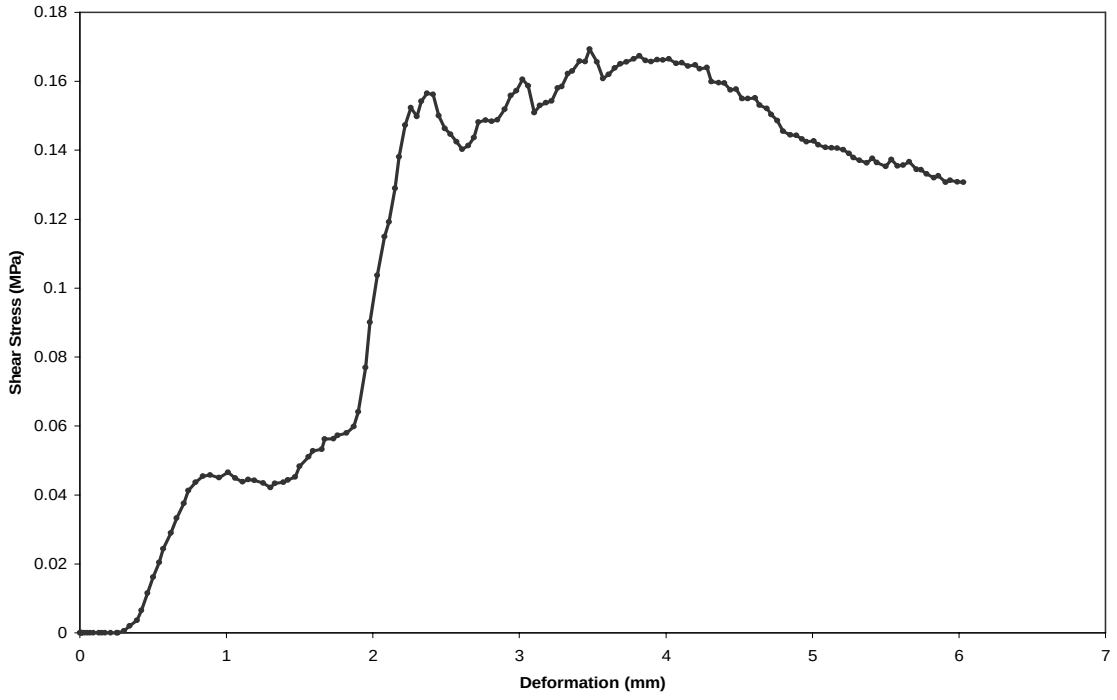

Fig 4.3 Deformation Vs Shear Stress for Type I Joint at 0.1 MPa Normal Stress for Sample C

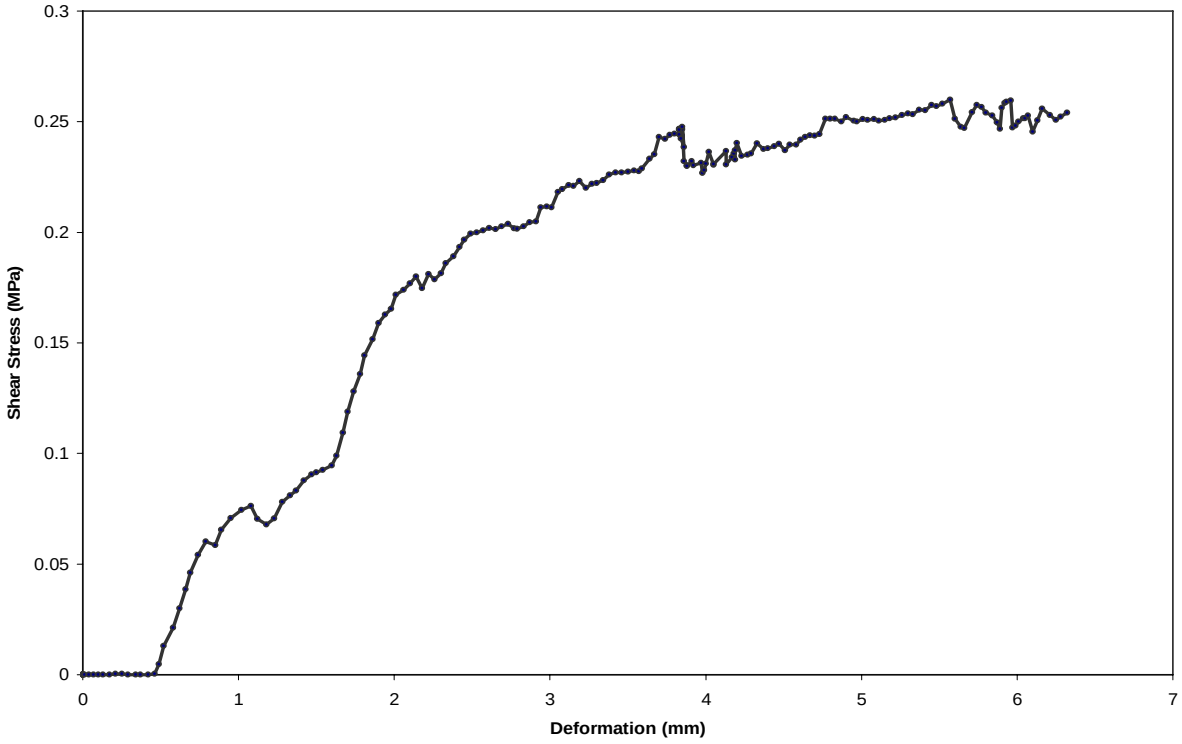

Fig 4.4 Deformation Vs Shear Stress for Type I Joint at 0.25 MPa Normal Stress for Sample A

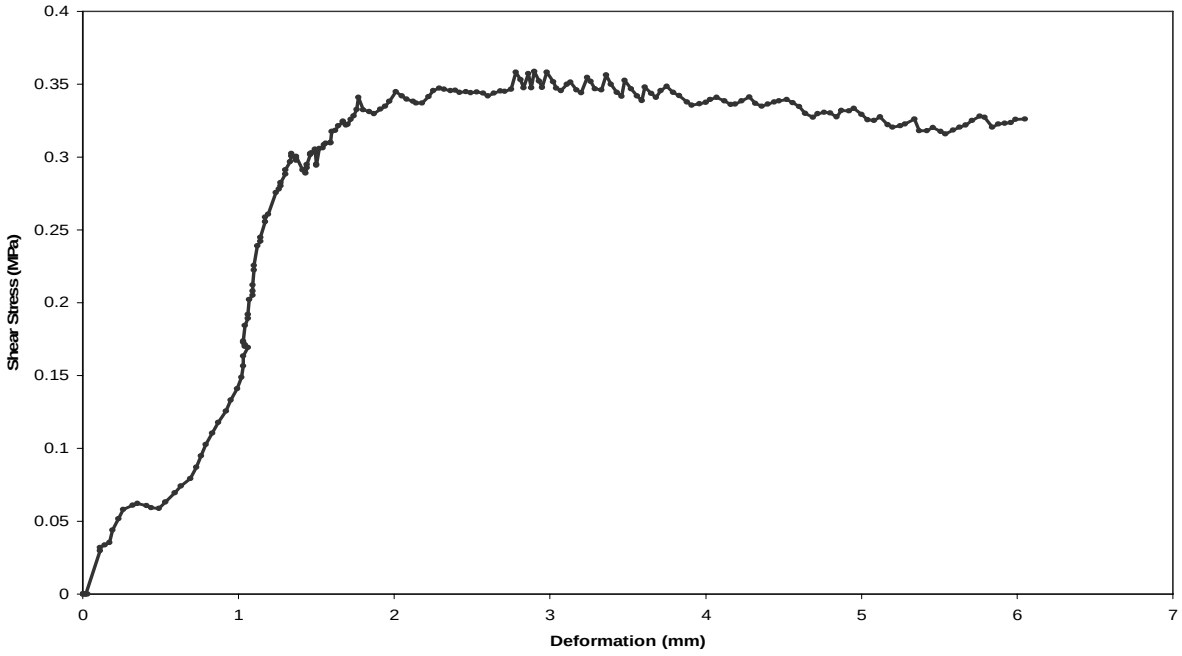

Fig 4.5 Deformation Vs Shear Stress for Type I Joint at 0.25 MPa Normal Stress for Sample B

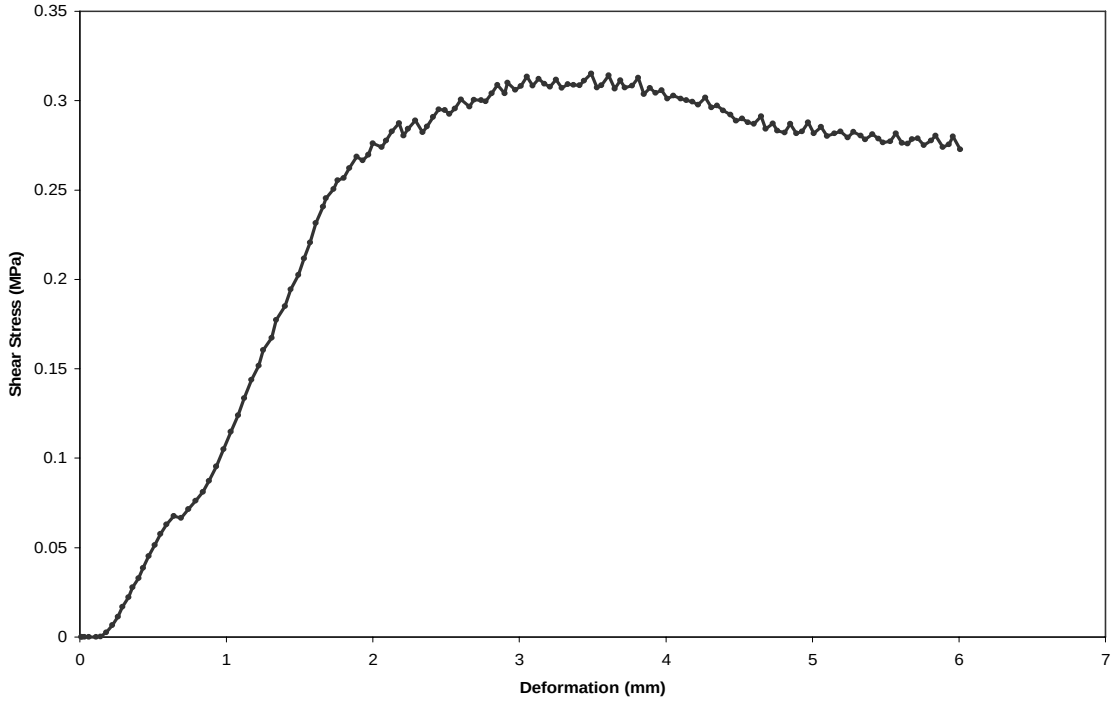

Fig 4.6 Deformation Vs Shear Stress for Type I Joint at 0.25 MPa Normal Stress for Sample C

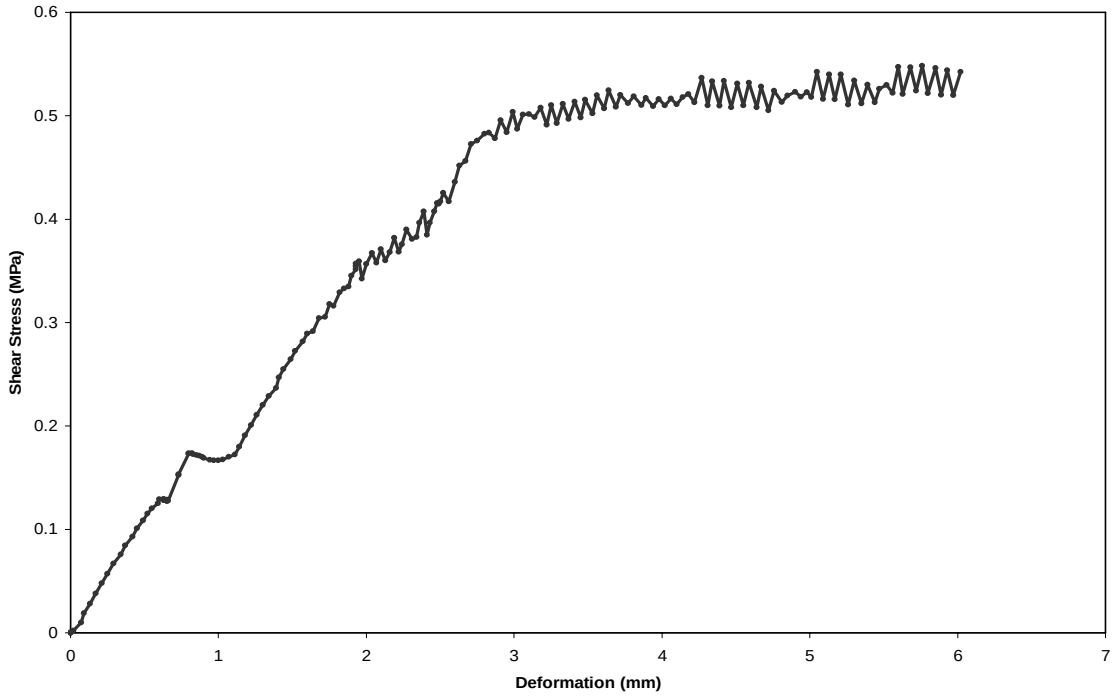

Fig 4.7 Deformation Vs Shear Stress for Type I Joint at 0.5 MPa Normal Stress for Sample A

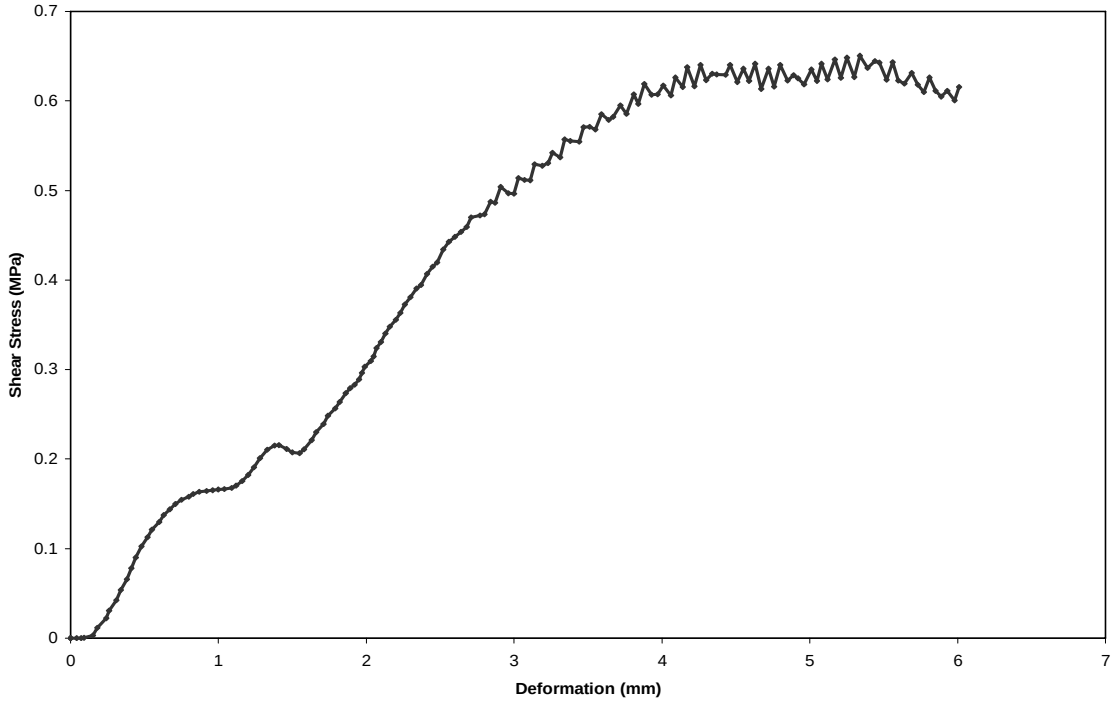

Fig 4.8 Deformation Vs Shear Stress for Type I Joint at 0.5 MPa Normal Stress for Sample B

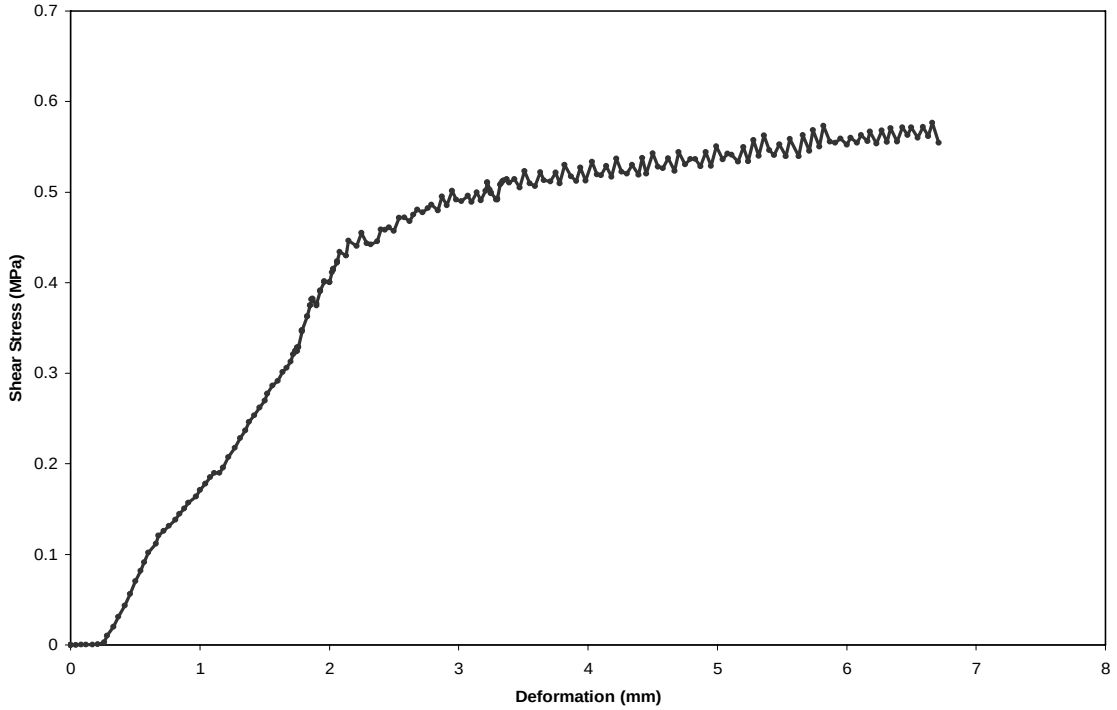

Fig 4.9 Deformation Vs Shear Stress for Type I Joint at 0.5 MPa Normal Stress for Sample C

Table 4.1 Shear Stiffness values for Type I Joint

Normal Stress (MPa)	Sample	Shear Stiffness (MPa/mm)
0.1	A	0.075
	B	0.053
	C	0.023
0.25	A	0.080
	B	0.049
	C	0.221
0.5	A	0.129
	B	0.106
	C	0.143

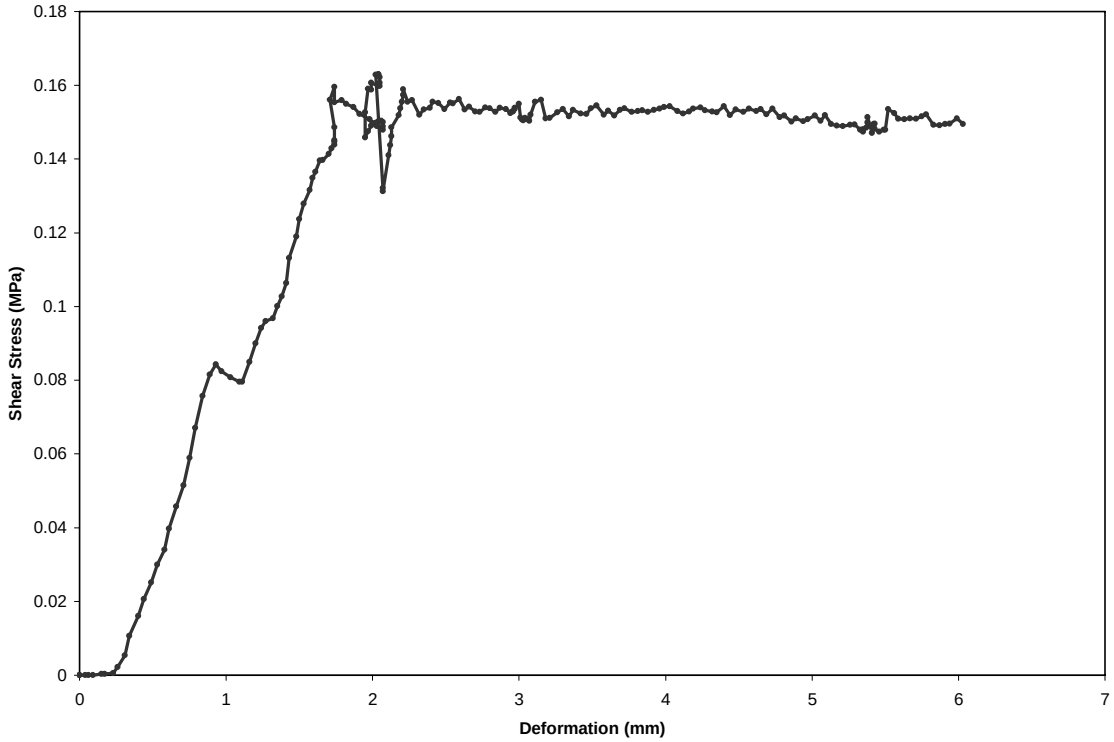

Fig 4.10 Deformation Vs Shear Stress for Type II Joint at 0.1 MPa Normal Stress for Sample A

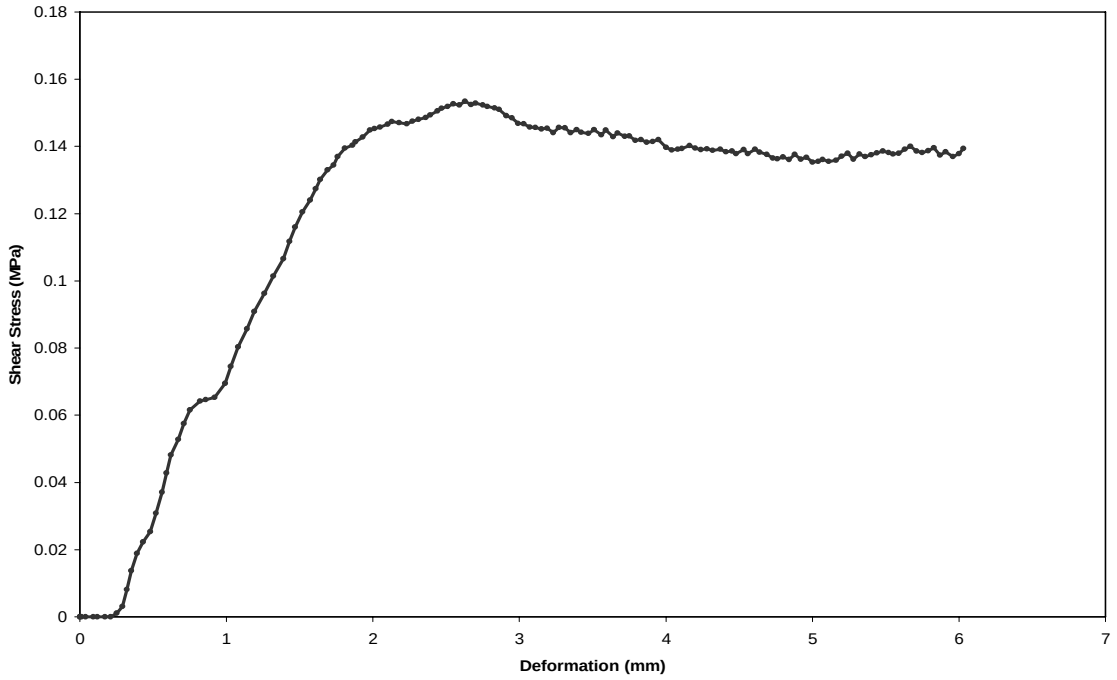

Fig 4.11 Deformation Vs Shear Stress for Type II Joint at 0.1 MPa Normal Stress for Sample B

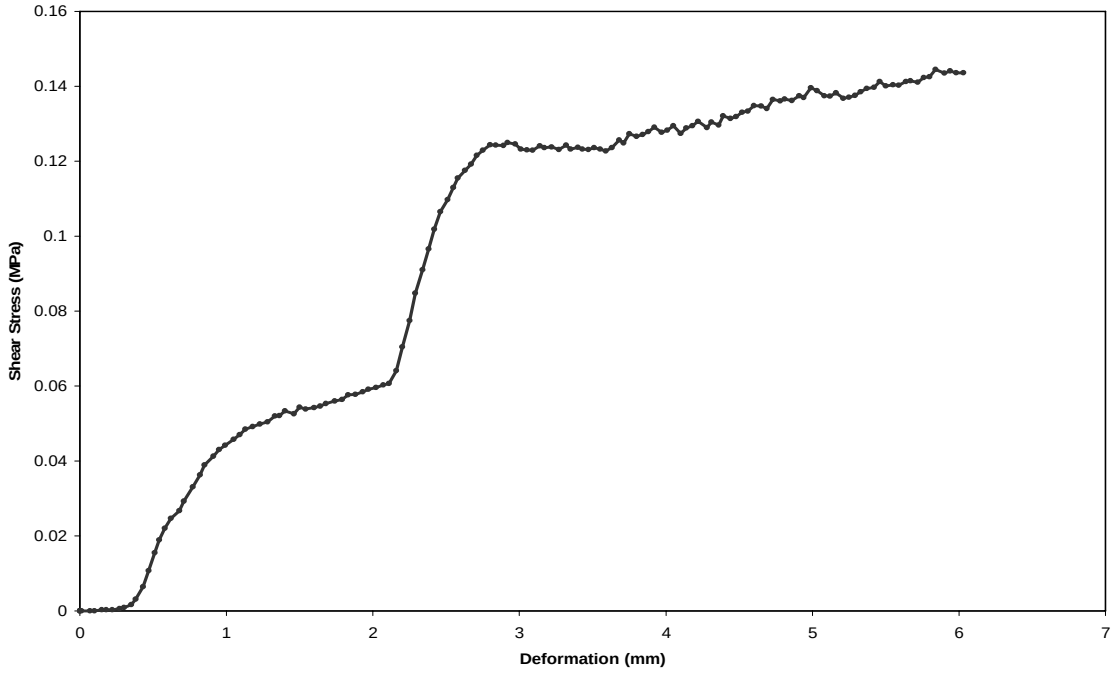

Fig 4.12 Deformation Vs Shear Stress for Type II Joint at 0.1 MPa Normal Stress for Sample C

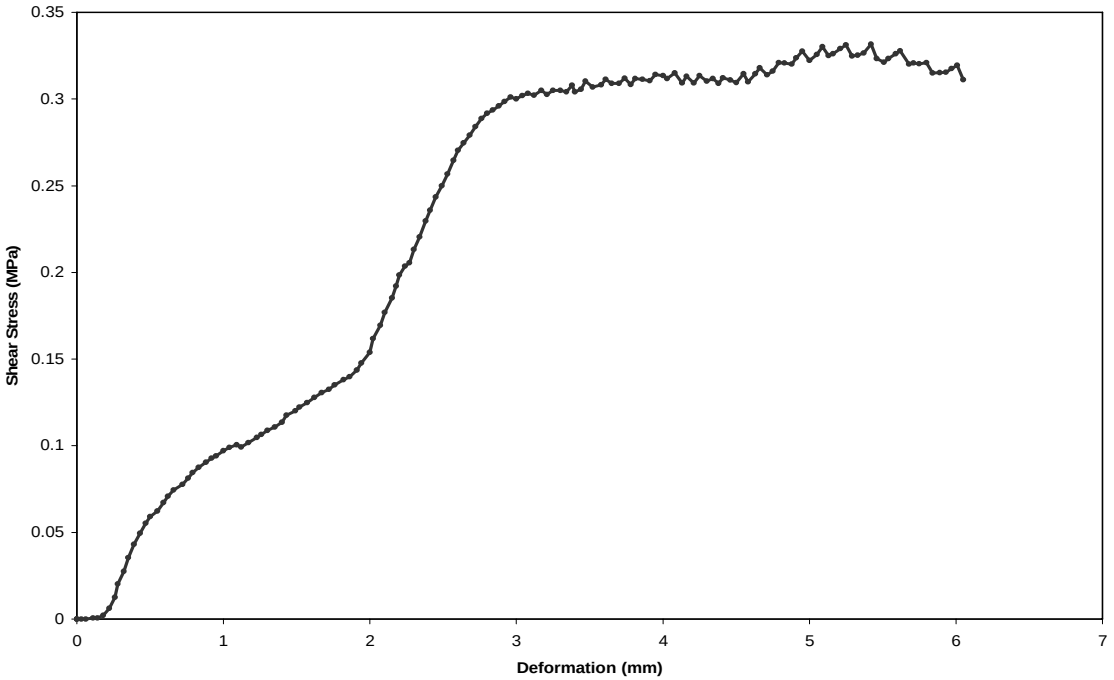

Fig 4.13 Deformation Vs Shear Stress for Type II Joint at 0.25 MPa Normal Stress for Sample A

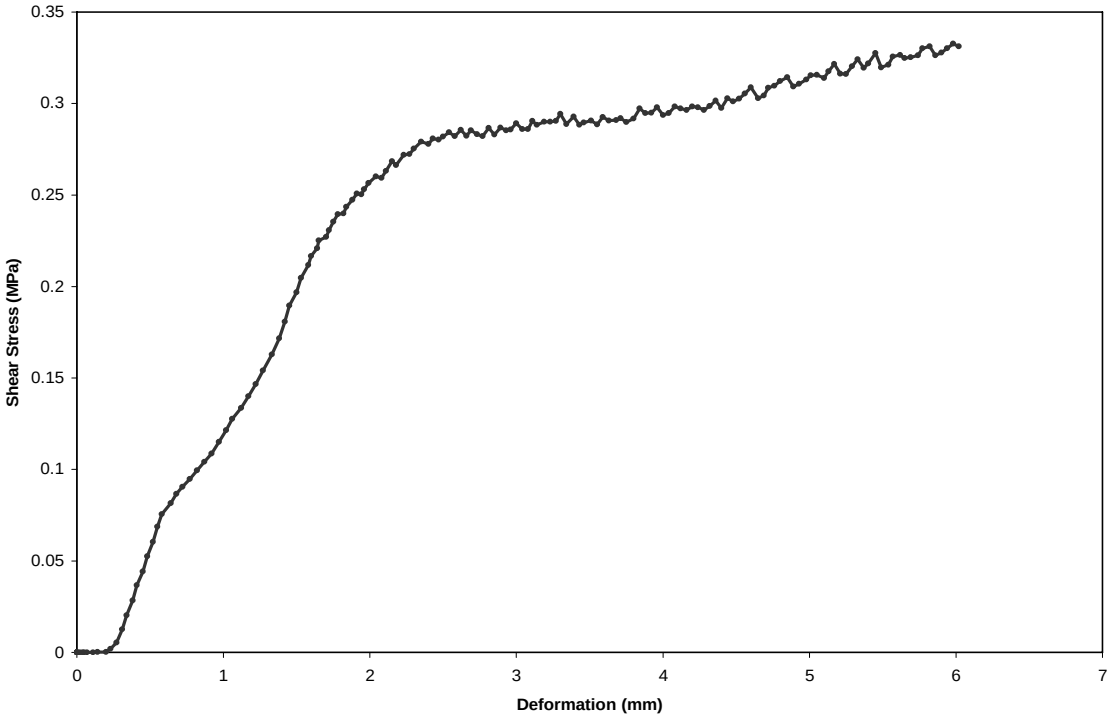

Fig 4.14 Deformation Vs Shear Stress for Type II Joint at 0.25 MPa Normal Stress for Sample B

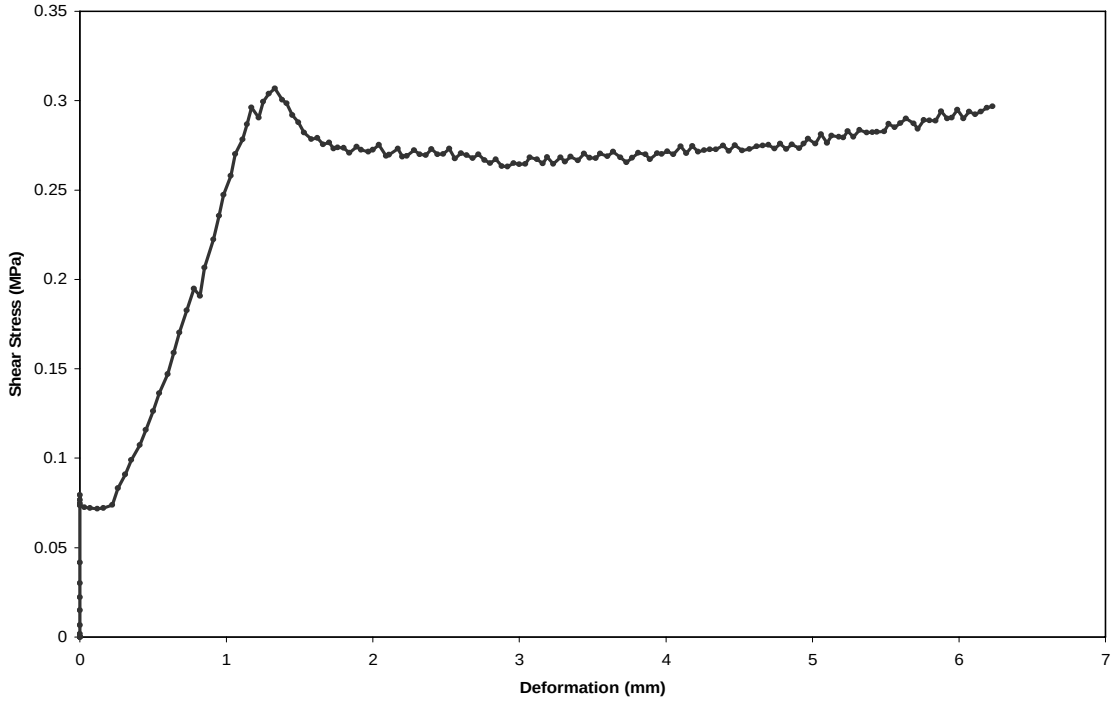

Fig 4.15 Deformation Vs Shear Stress for Type II Joint at 0.25 MPa Normal Stress for Sample C

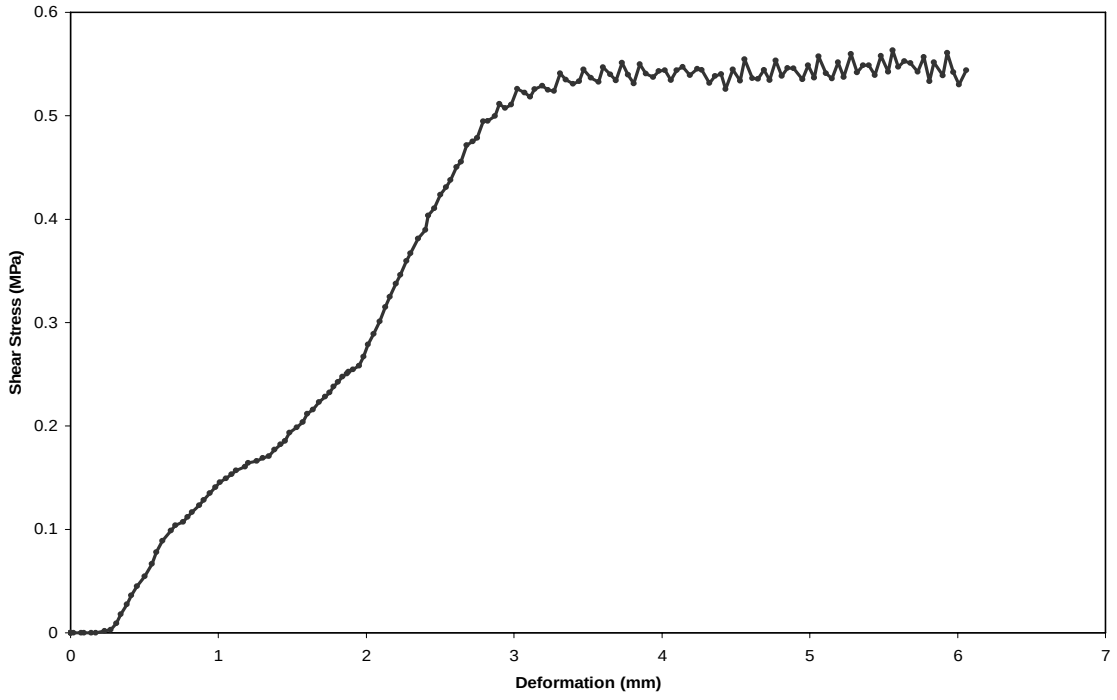

Fig 4.16 Deformation Vs Shear Stress for Type II Joint at 0.5 MPa Normal Stress for Sample A

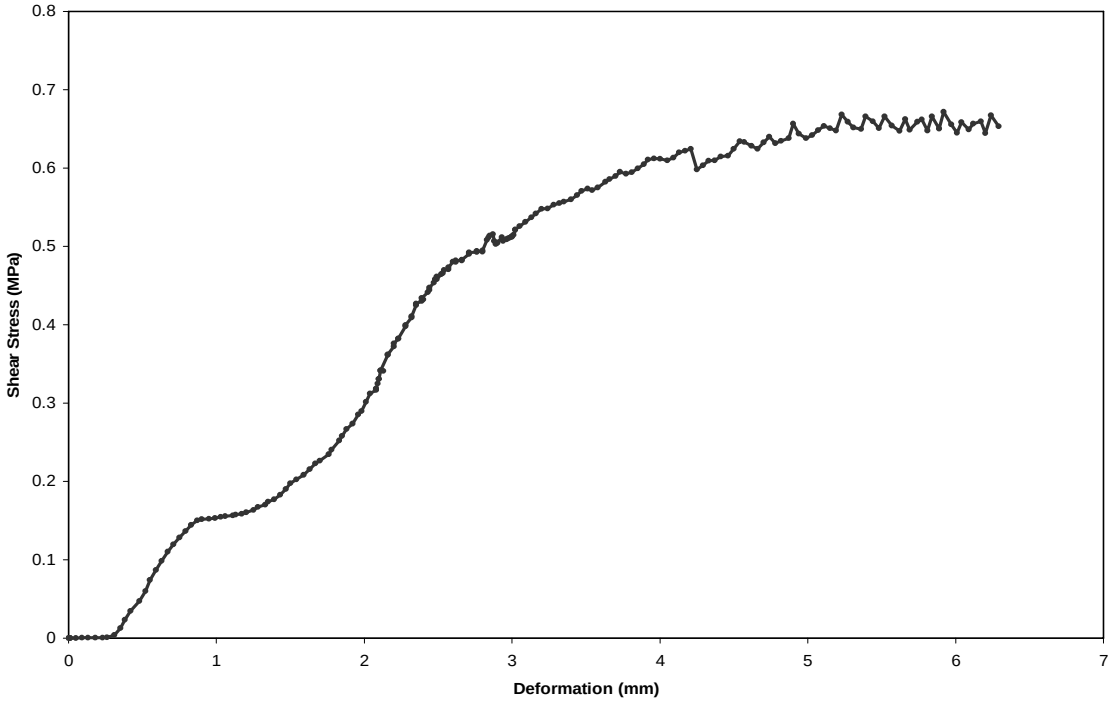

Fig 4.17 Deformation Vs Shear Stress for Type II Joint at 0.5 MPa Normal Stress for Sample B

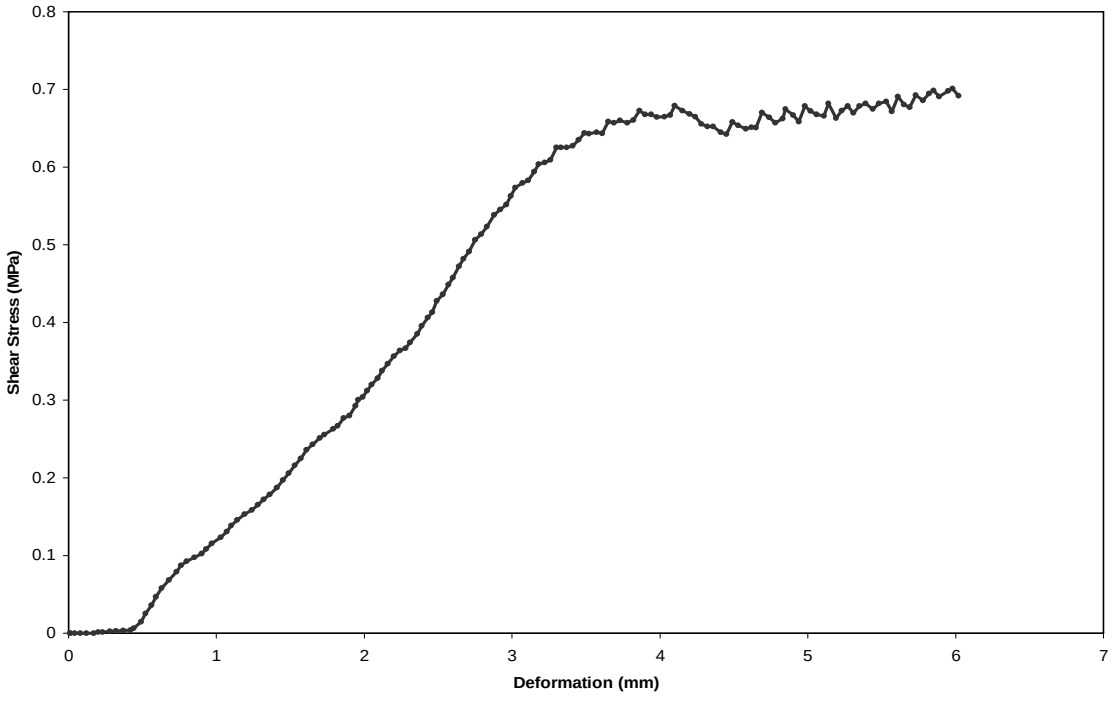

Fig 4.18 Deformation Vs Shear Stress for Type II Joint at 0.5 MPa Normal Stress for Sample C

Table 4.2 Shear Stiffness values for Type II Joint

Normal Stress (Mpa)	Sample	Shear Stiffness (MPa/mm)
0.1	A	0.044
	B	0.037
	C	0.043
0.25	A	0.056
	B	0.117
	C	0.092
0.5	A	0.127
	B	0.129
	C	0.122

Once shear stiffness for different normal stresses are known a relation can be developed between normal stress (σ_n) and shear stiffness (k_s). In present study an exponential relation is derived using MATLAB 7.0 for Type I and Type II joint. Relation for Type I joint is shown in Fig. 4.19 while for Type II joint, relation is shown in Fig. 4.20.and combining they are shown in Fig 4.21.

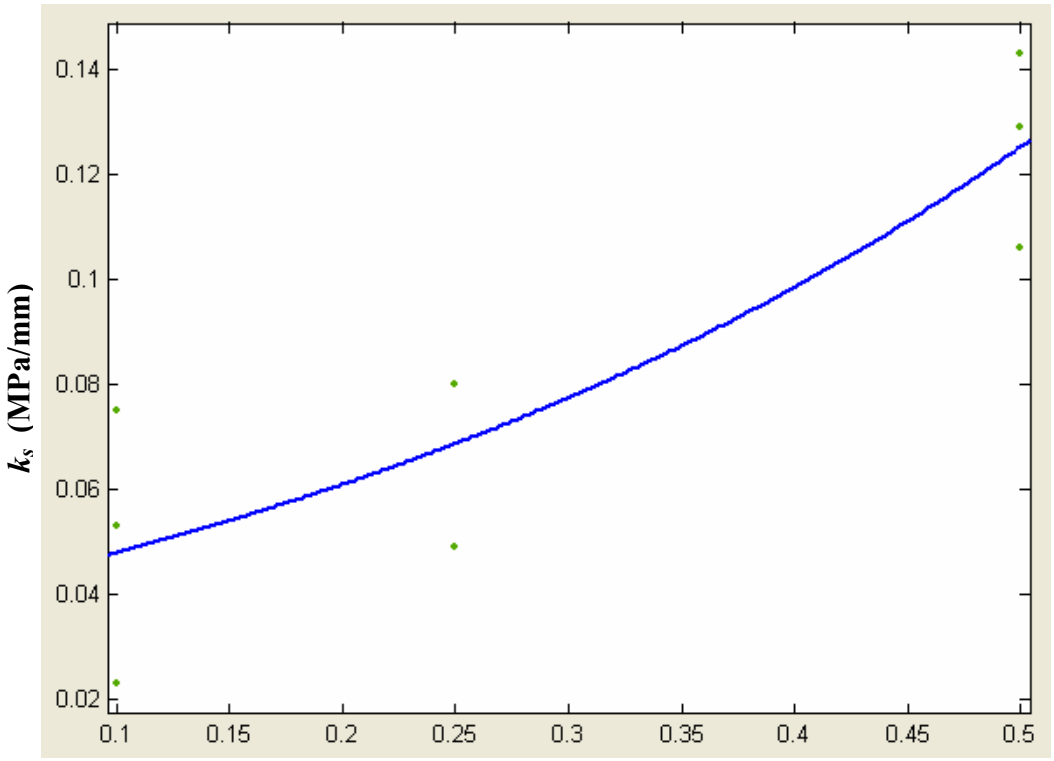

Fig. 4.19 Relation between σ_n & k_s for Type I Joint

Equation for above relation obtained is of the form.

$$k_s = a \times e^{b\sigma_n} \qquad (4.1)$$

Where, a = 0.0376

b = 2.410

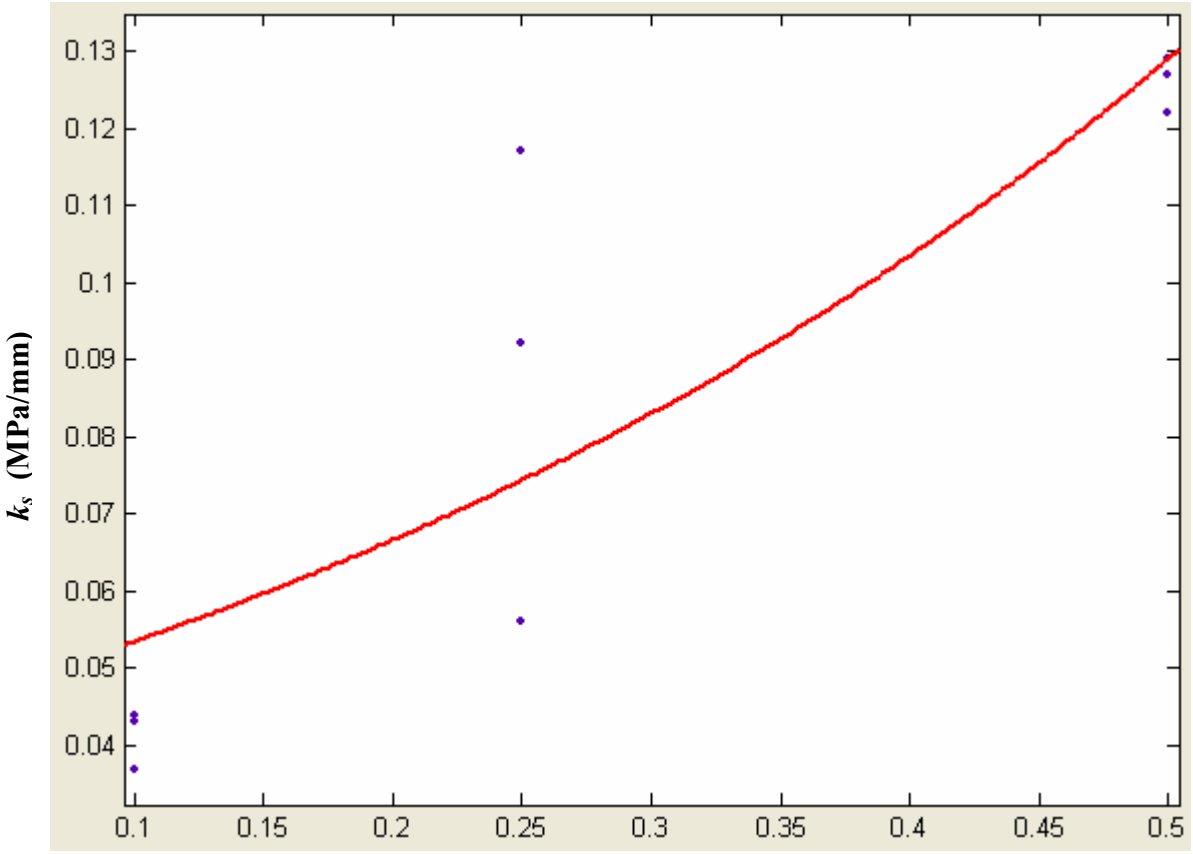

Fig. 4.20 Relation between σ_n & k_s for Type II Joint

Equation for above relation obtained is

$$k_s = a' \times e^{b'\sigma_n} \qquad (4.2)$$

Where, a' = 0.04291

b' = 2.201

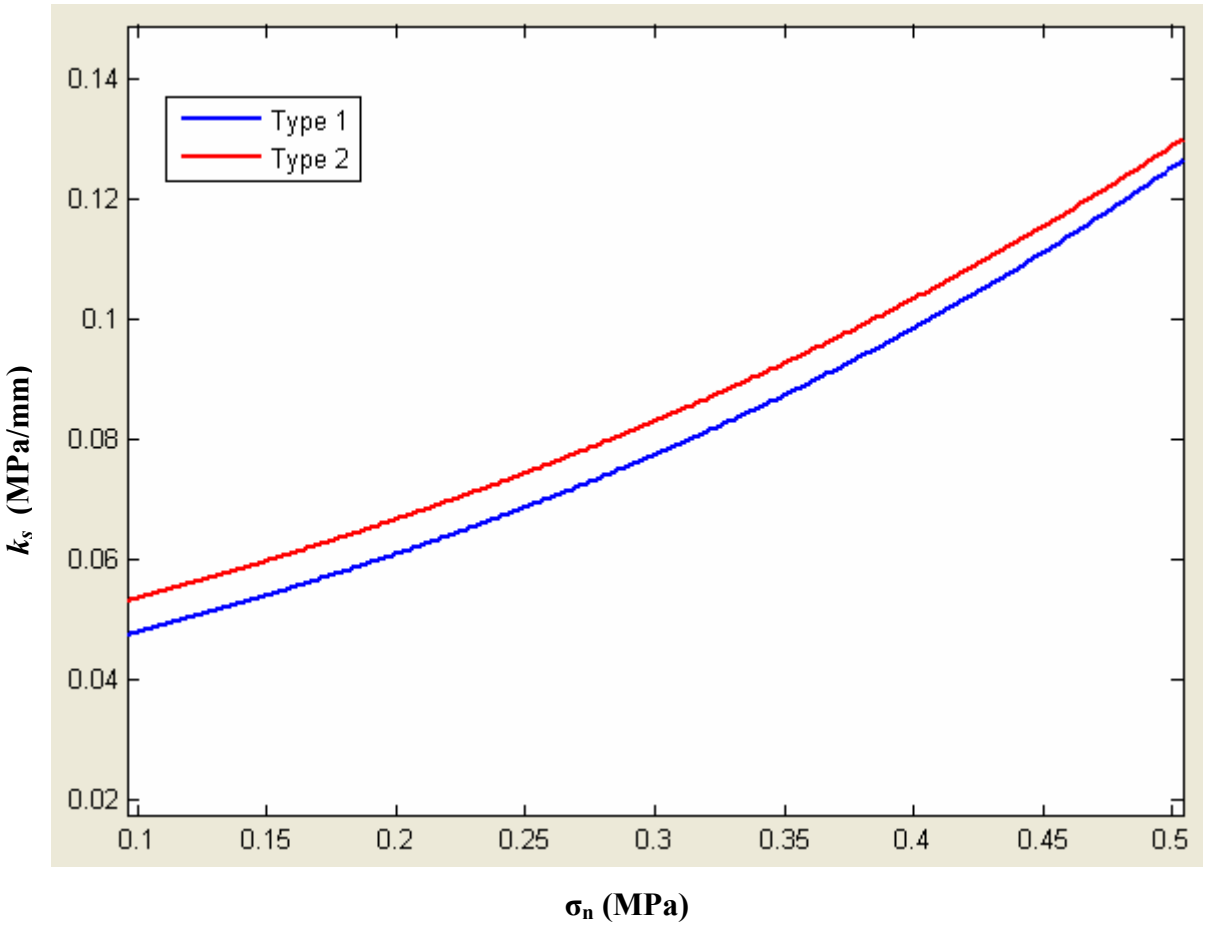

Fig. 4.21 Relation between σ_n & k_s for both Type I and Type II Joint

Natural joint (Type I) is the joint normally found, and the departure of the Hacksaw joint (Type II) from Natural joint can be given as

$$\frac{a}{a'} = 0.8763 \quad \text{and} \quad \frac{b}{b'} = 1.0950$$

4.1.2 Normal Stiffness

1. **Type I Joint:** Specimens having naturally broken joints were tested under compressive testing machine. Three samples named as Sample A, B & C for each number of joints i.e. specimen having single, double, three and four were tested. The observed normal stresses against deformations have been shown in Fig. 4.22

to Fig. 4.25. Value of normal stiffness for different no of joints for all three samples along with their average value is reported in Table 4.3. Average value is obtained by plotting reading of all three samples simultaneously for each number of joints. Plot is shown in Fig. 4.26 to Fig. 4.29. For single joint normal stiffness value varies from 2.09 to 2.25 MPa/mm. For double joint the value varies from 1.43 to 1.90 MPa/mm. While the range is 2.88 to 4.84 MPa/mm and 2.20 to 3.83 MPa/mm for three and four number of joints respectively.

2. **Type II Joint:** Deformation Vs normal stiffness (k_n) plot for Type II joint in all four cases of number of joints is shown in Fig. 4.30 to Fig. 4.33. The normal stiffness value is tabulated in Table 4.4. Single joint specimens show a variation of 2.47 to 3.07 MPa/mm in normal stiffness values. This range is 3.87 to 6.39 Mpa/mm and 2.88 to 4.84 MPa/mm for double and triple joints respectively. For sample having four joints the values noted was from 2.20 to 3.83 MPa/mm. Plots to obtain average value of normal stiffness is shown in Figs. 4.34 to 4.37.

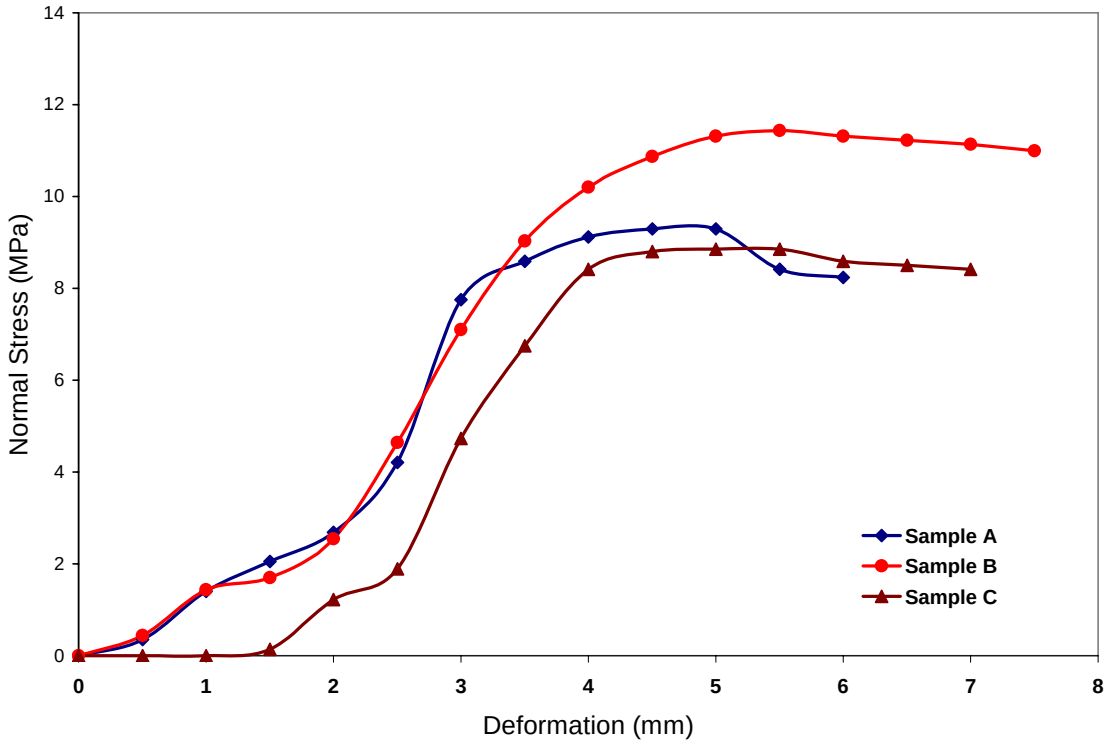

Fig. 4.22 Deformation Vs Normal Stress for Type I - One Joint

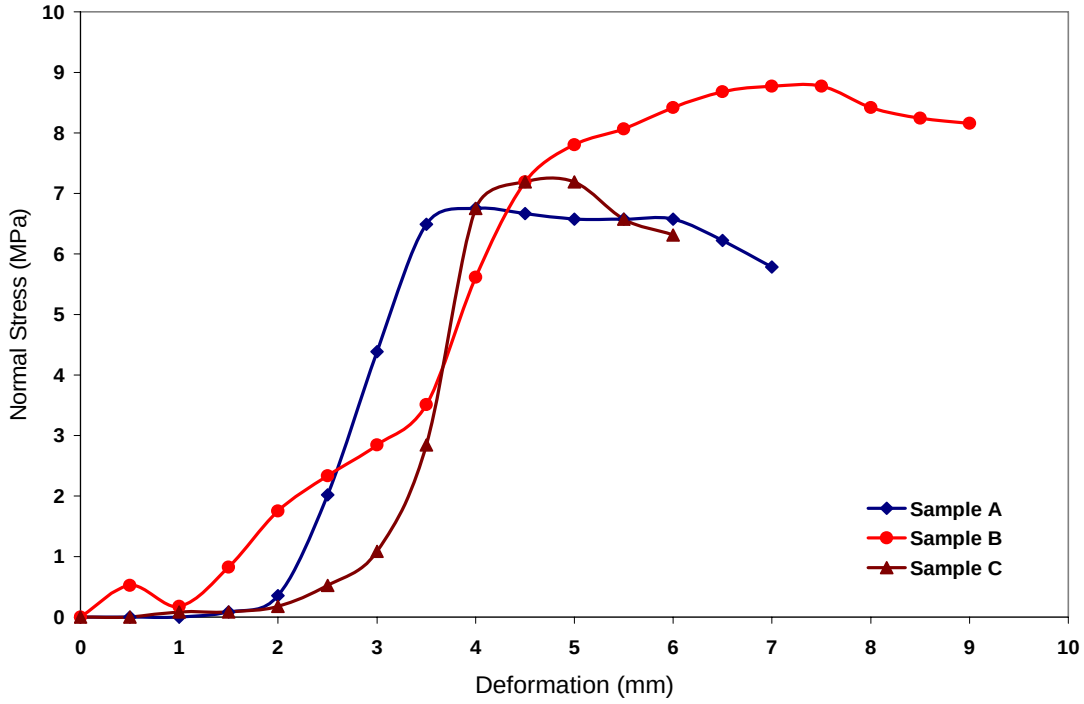

Fig. 4.23 Deformation Vs Normal Stress for Type I - Two Joints

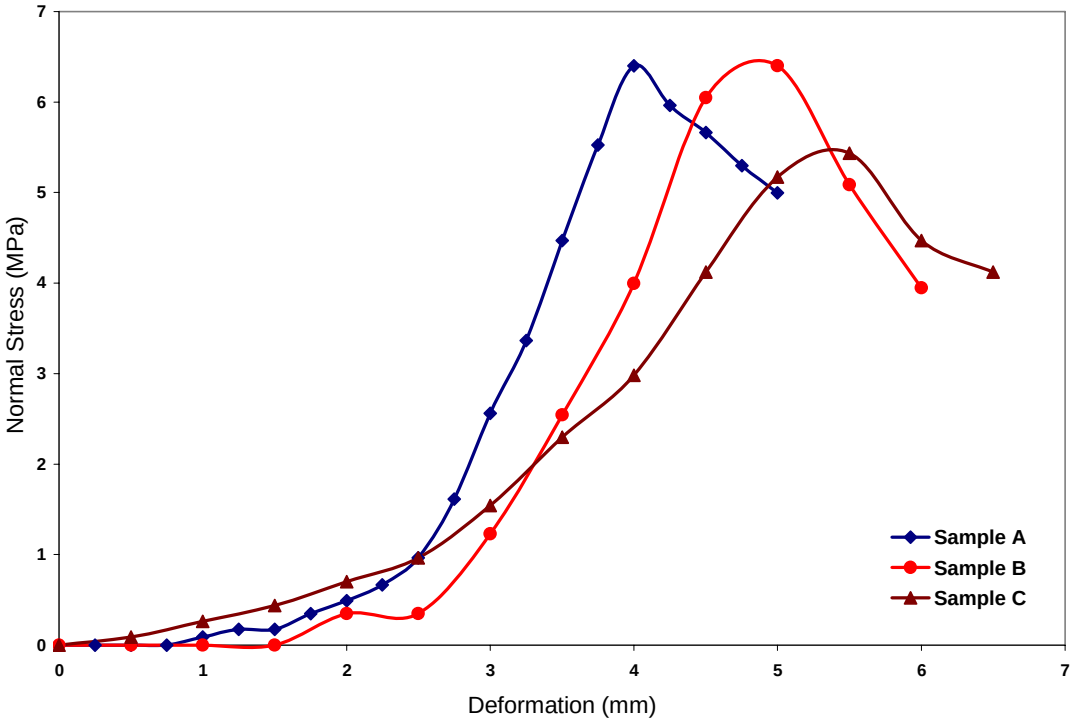

Fig. 4.24 Deformation Vs Normal Stress for Type I - Three Joints

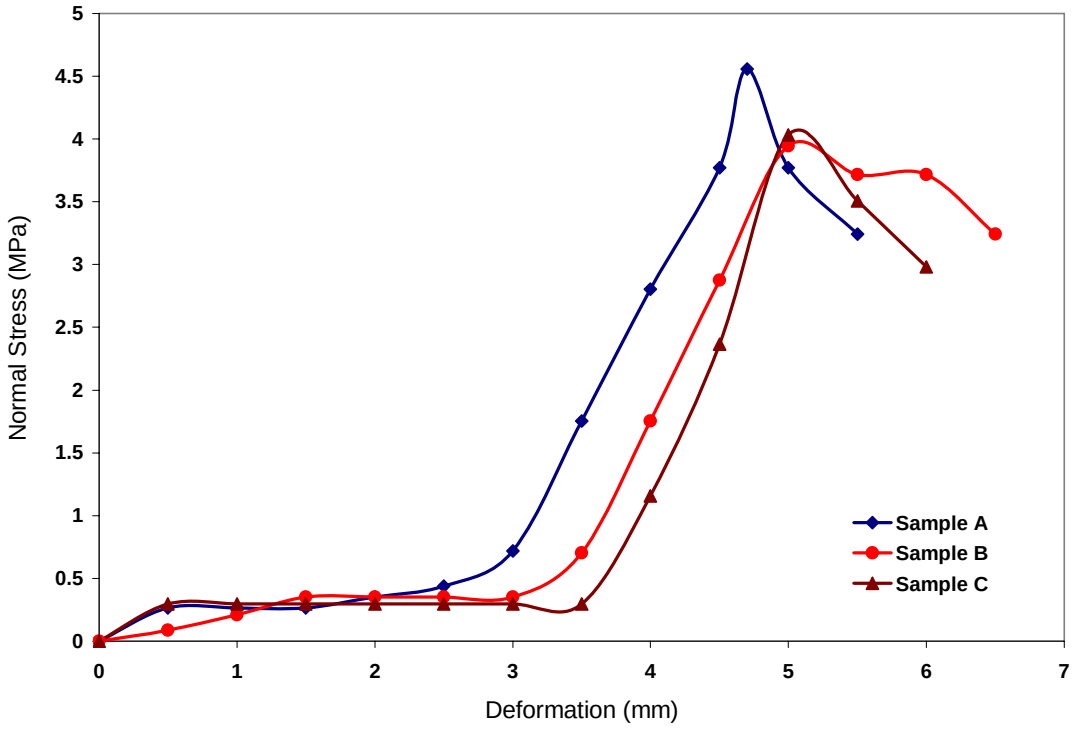

Fig. 4.25 Deformation Vs Normal Stress for Type I - Four Joints

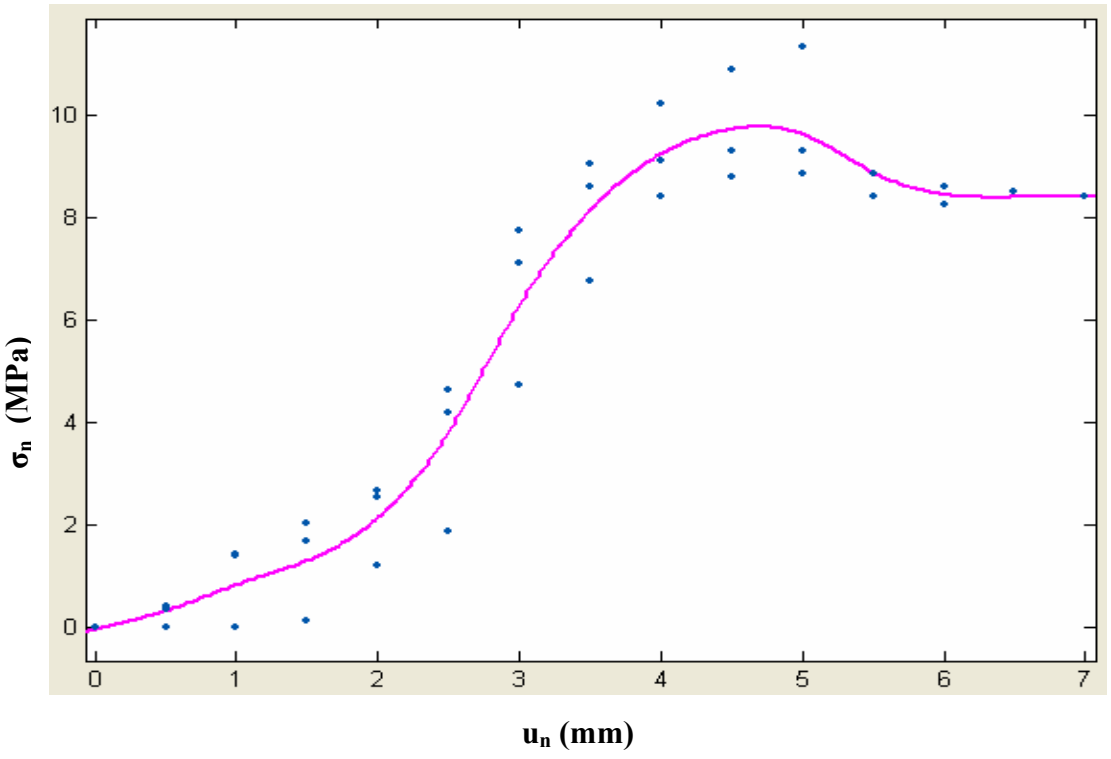

Fig. 4.26 Estimating Average Normal Stiffness for Type I – One Joint

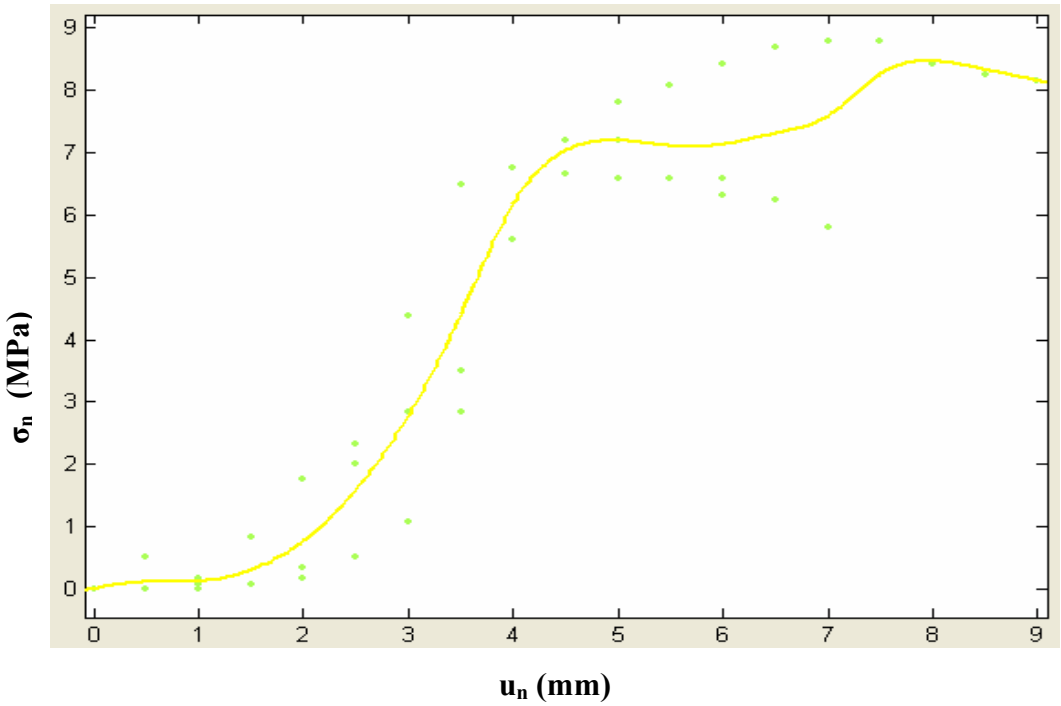

Fig. 4.27 Estimating Average Normal Stiffness for Type I – Two Joints

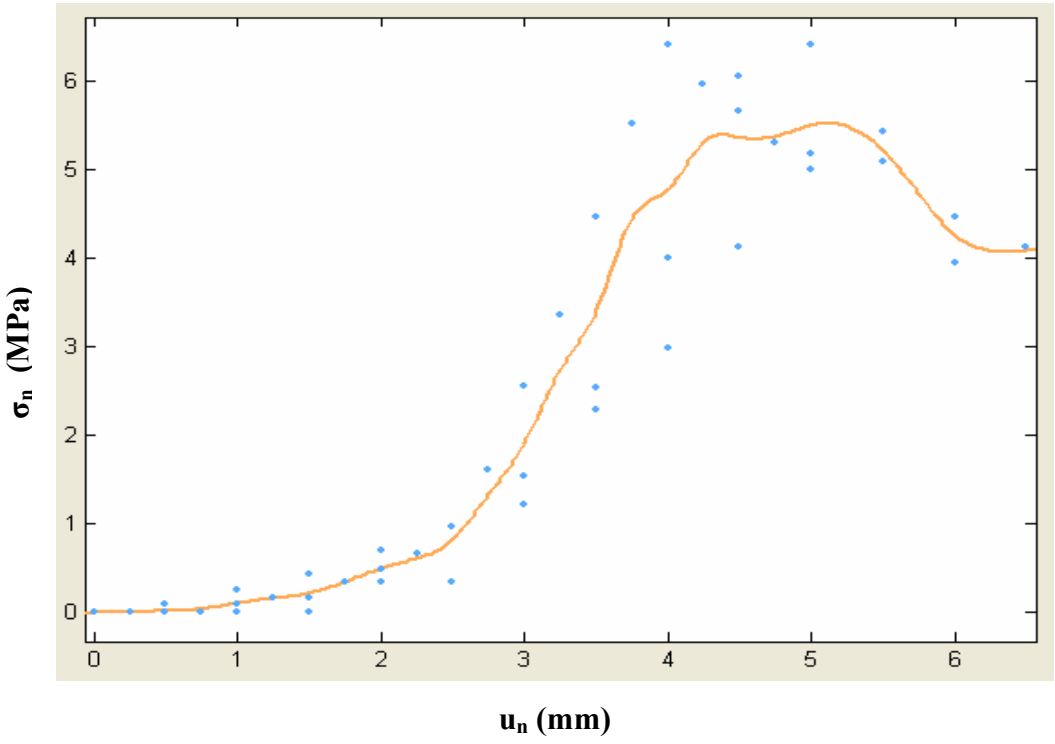

Fig. 4.28 Estimating Average Normal Stiffness for Type I – Three Joints

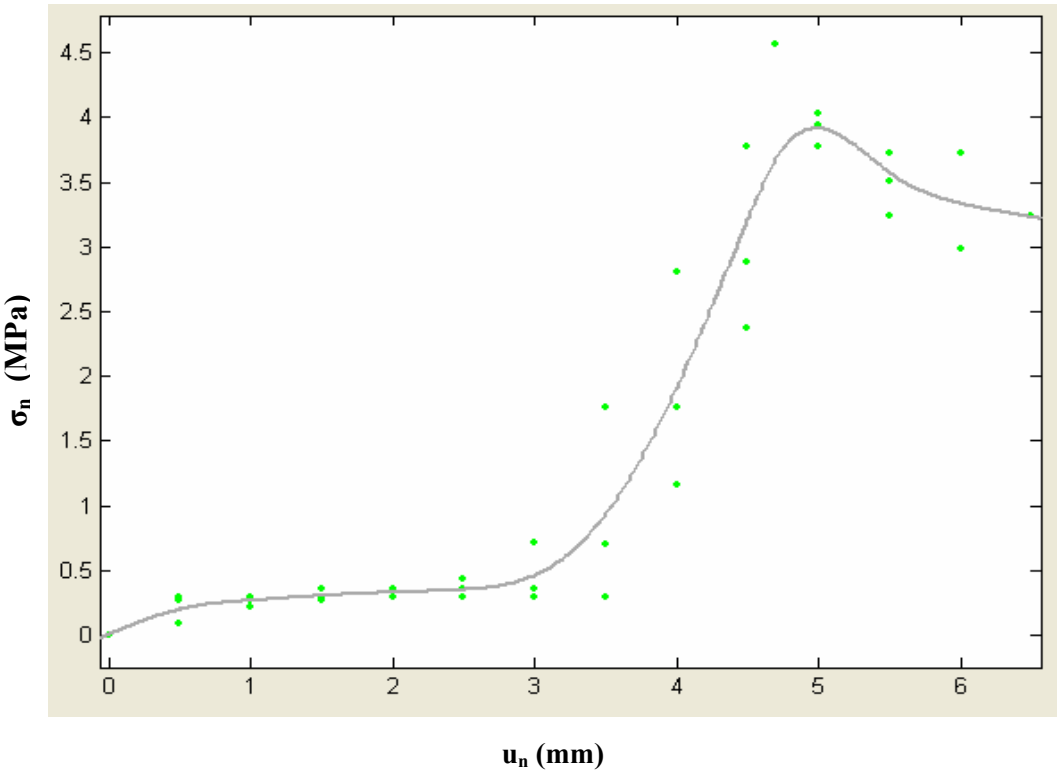

Fig. 4.29 Estimating Average Normal Stiffness for Type I – Four Joint

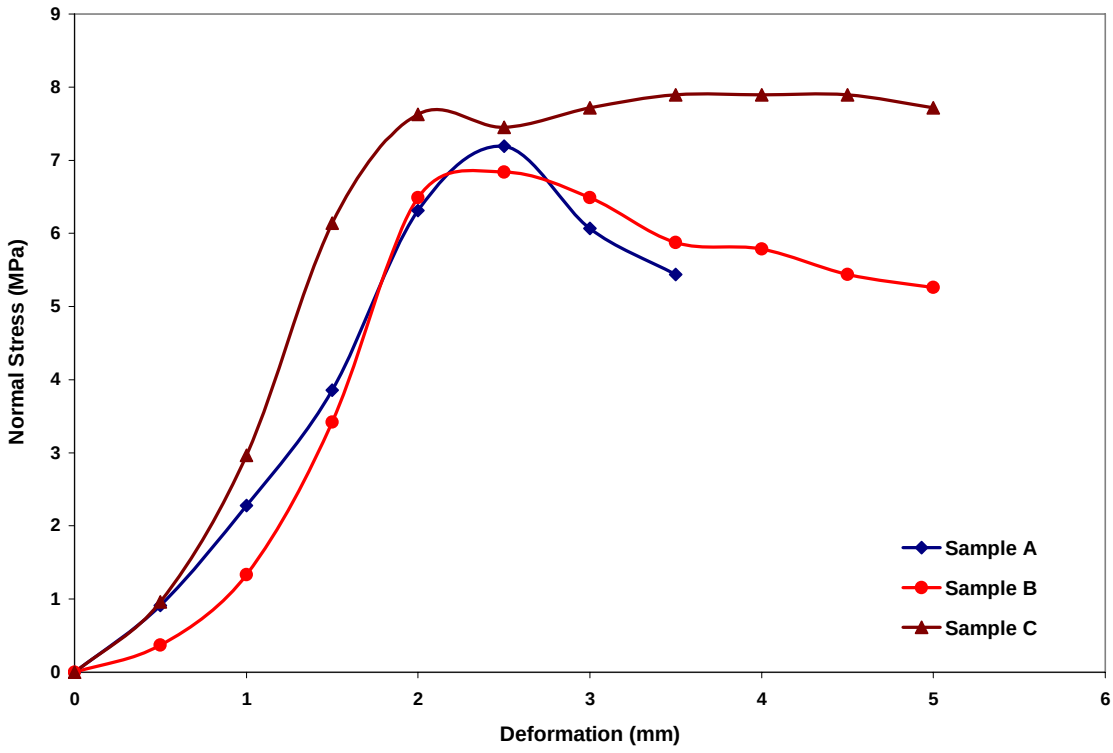

Fig. 4.30 Deformation Vs Normal Stress for Type II - One Joint

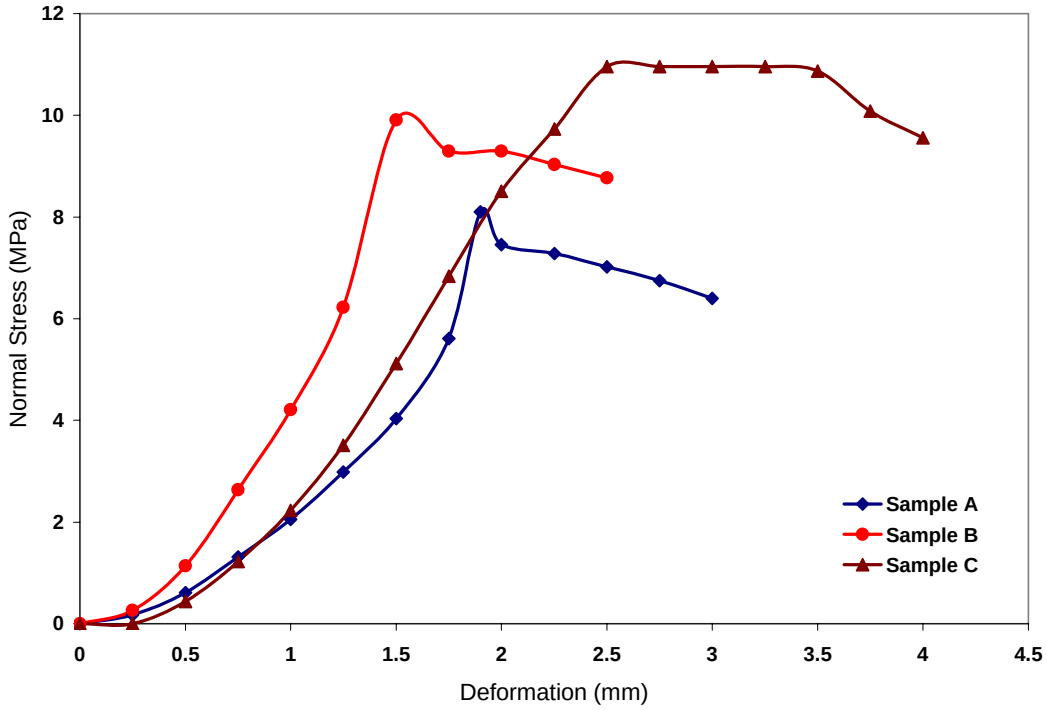

Fig. 4.31 Deformation Vs Normal Stress for Type II - Two Joints

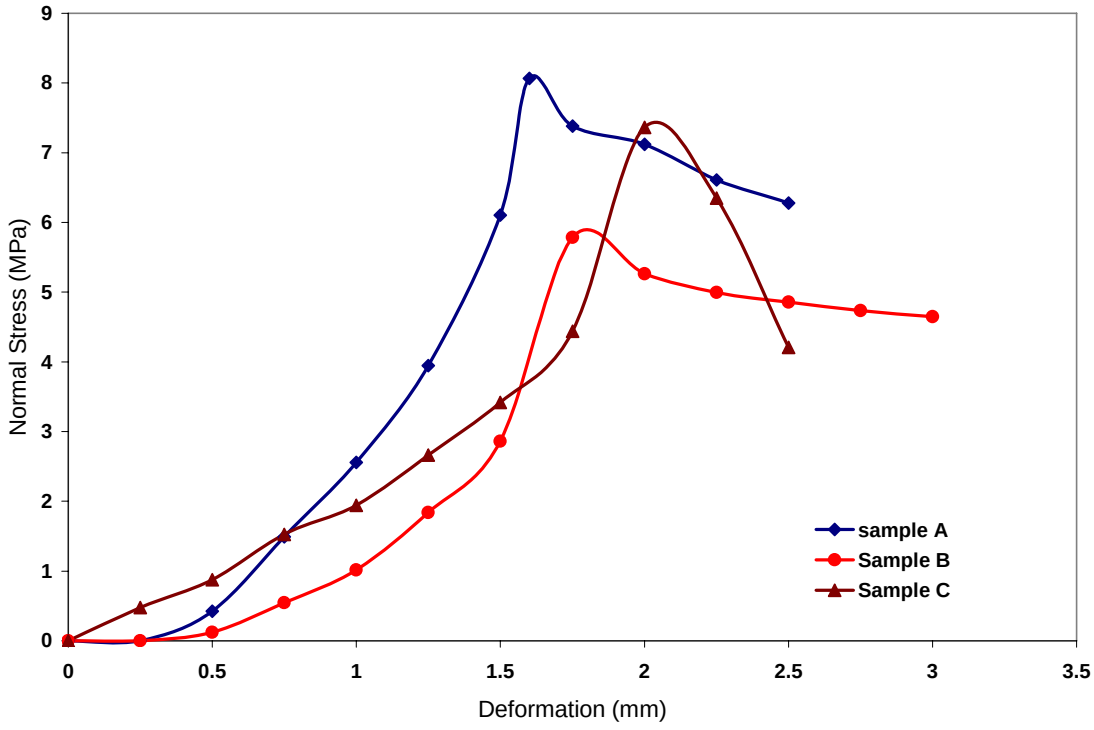

Fig. 4.32 Deformation Vs Normal Stress for Type II -Three Joints

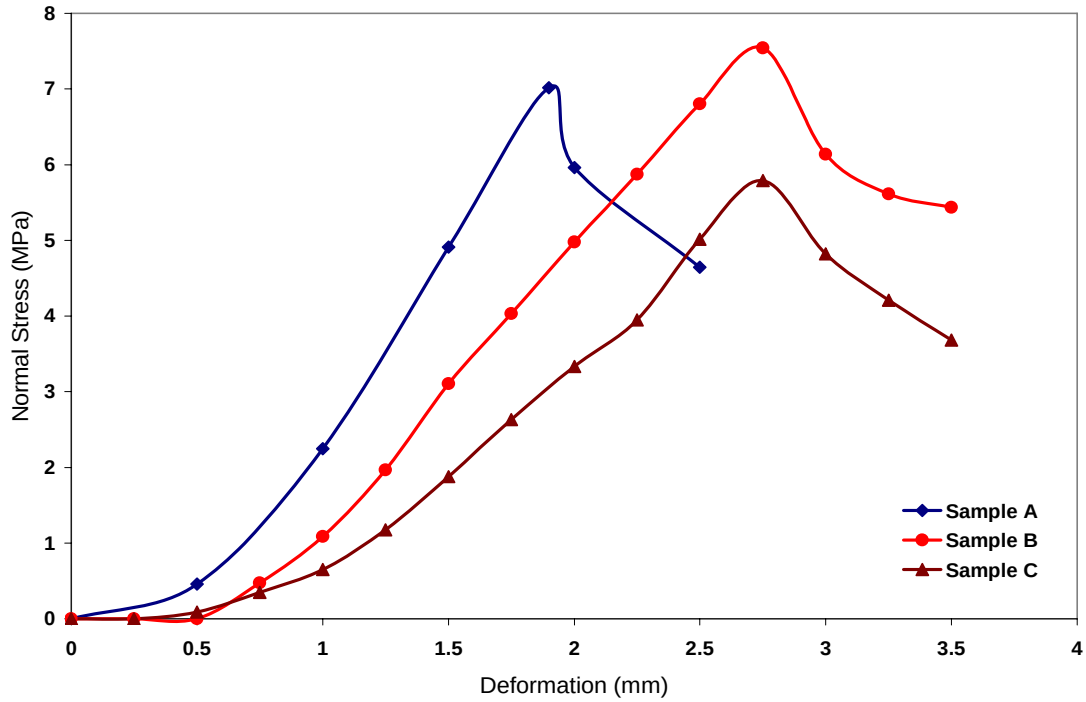

Fig. 4.33 Deformation Vs Normal Stress for Type II - Four Joints

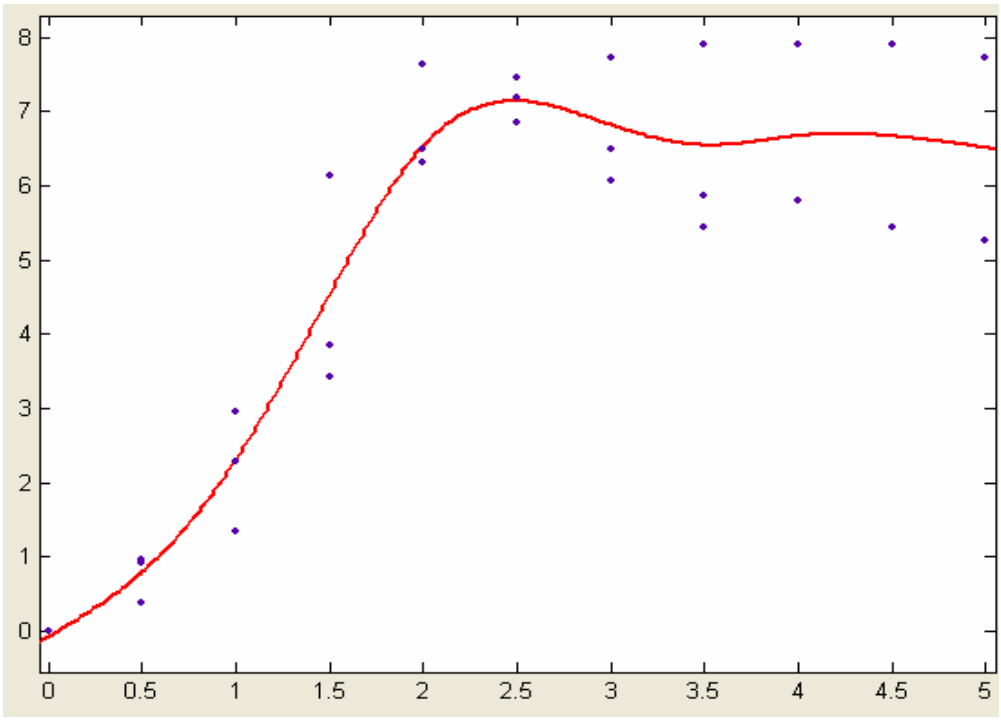

Fig. 4.34 Estimating Average Normal Stiffness for Type II - One Joint

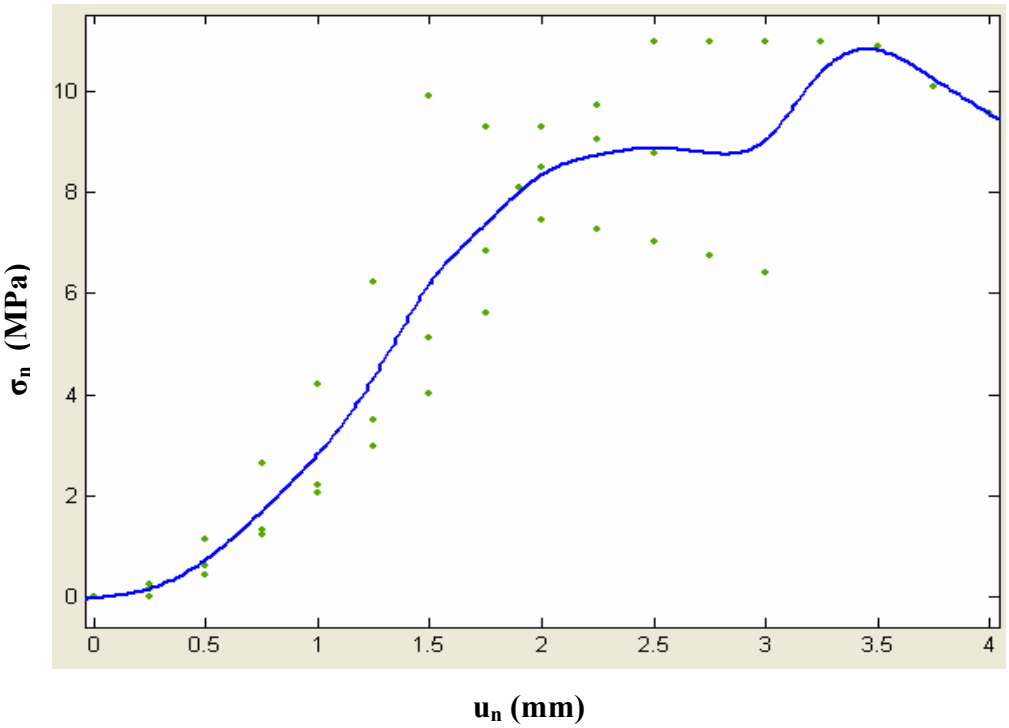

Fig. 4.35 Estimating Average Normal Stiffness for Type II -Two Joints (u_n Vs σ_n)

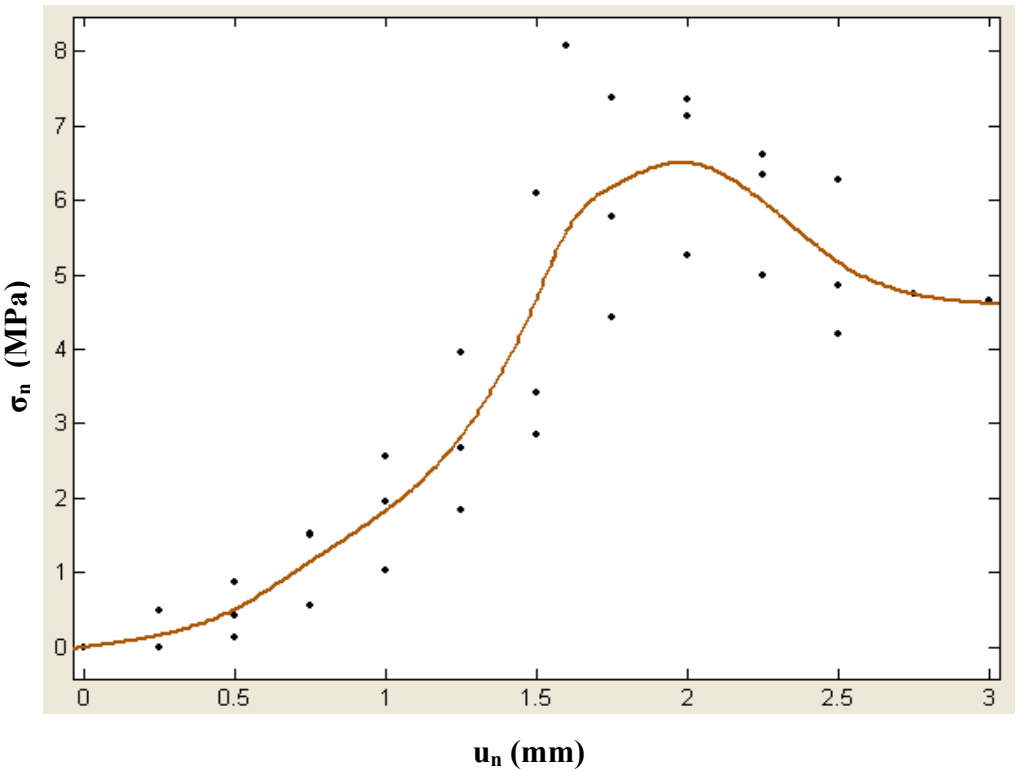

Fig. 4.36 Estimating Average Normal Stiffness for Type II -Three Joints (u_n Vs σ_n)

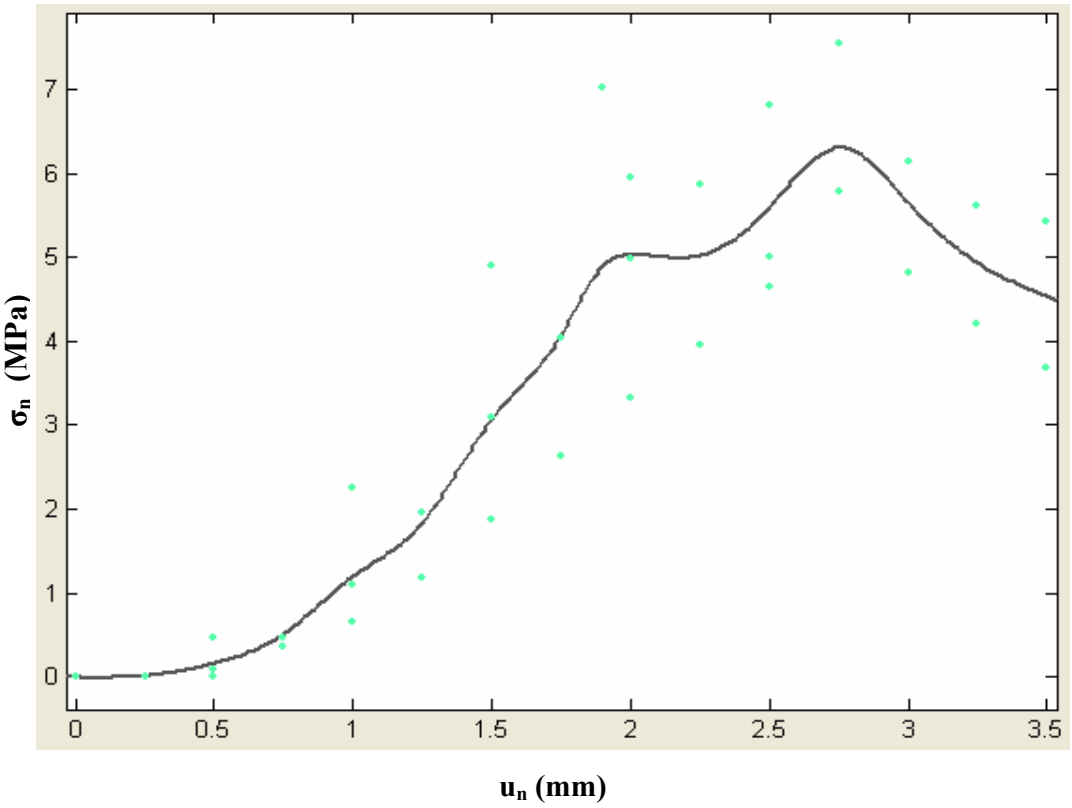

Fig. 4.37 Estimating Average Normal Stiffness for Type II -Four Joints

Table 4.3 Normal Stiffness Values for Type I Joint

No of Joints	Normal Stiffness (MPa/mm)			Average Normal Stiffness (MPa/mm)
	Sample A	Sample B	Sample C	
One	2.25	2.48	2.09	2.28
Two	1.90	1.43	1.66	1.58
Three	1.47	1.34	1.05	1.23
Four	0.88	0.66	0.56	0.69

Table 4.4 Normal Stiffness Values for Type II Joint

No of Joints	Normal Stiffness (MPa/mm)			Average Normal Stiffness (MPa/mm)
	Sample A	Sample B	Sample C	
One	3.07	3.12	1.8	2.22
Two	3.87	6.39	4.22	4.17
Three	4.84	2.88	3.17	3.70
Four	3.83	3.05	2.20	3.65

4.2 ESTIMATION OF c & φ

Mohr – Coulomb gave the famous relation consisting shear strength (τ), normal stress (σ_n), cohesion (c) and angle of repose (φ) for soil mass. The relation is

$$\tau = c + \sigma_n \tan\varphi \qquad (4.3)$$

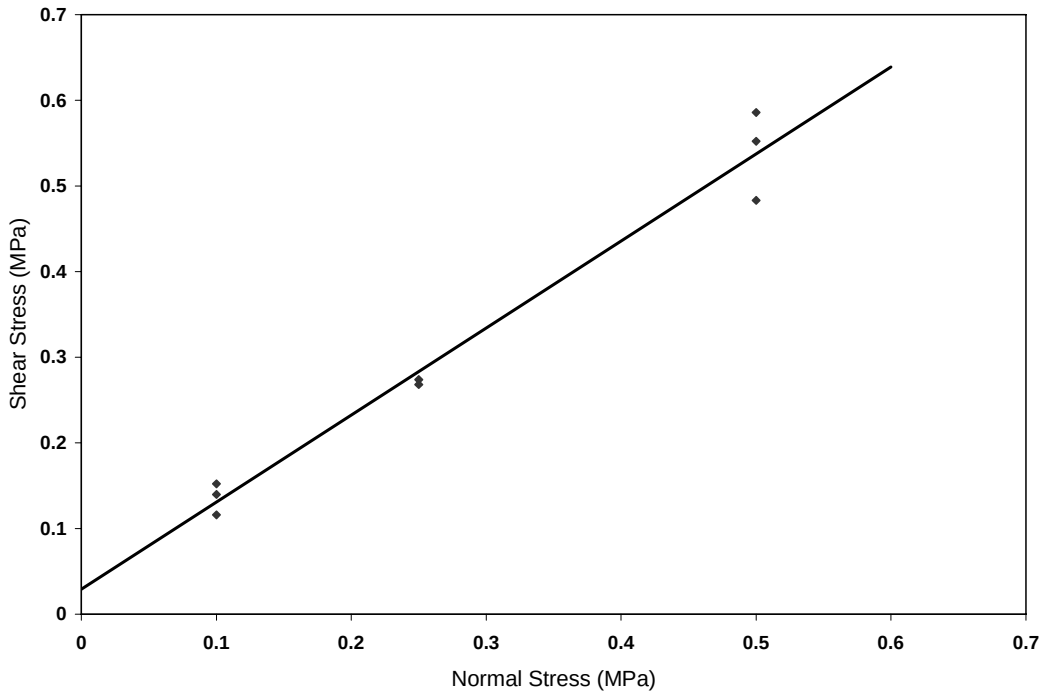

Fig 4.38 Estimation of c & φ for Type I Joint

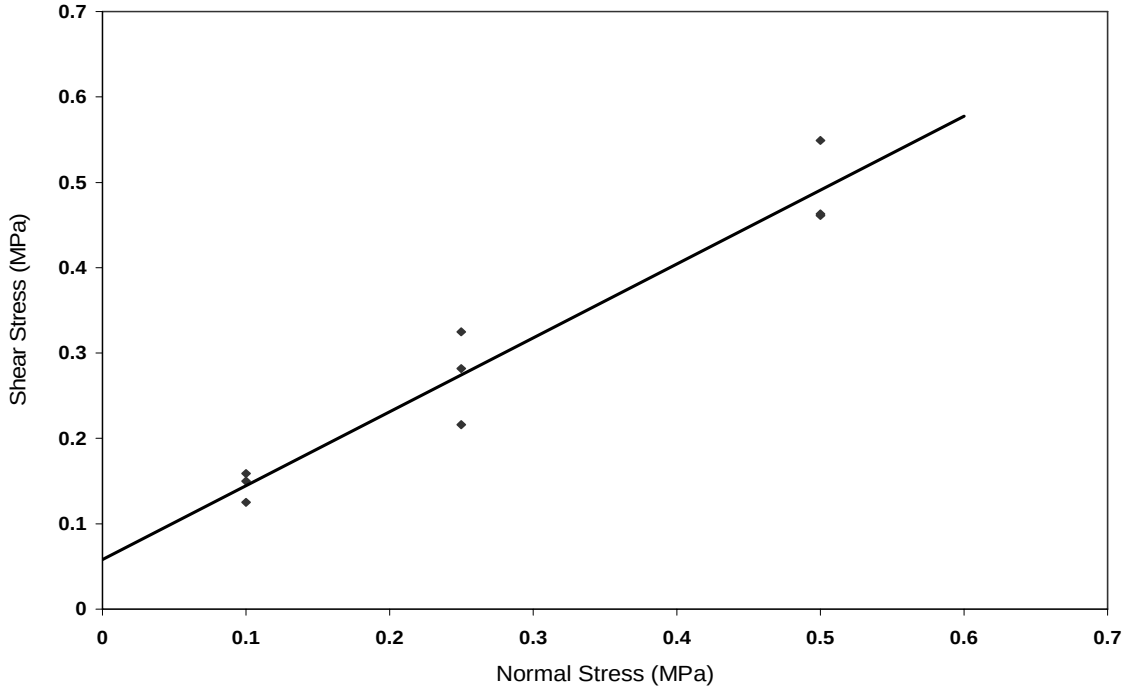

Fig 4.39 Estimation of c & φ for Type II Joint

Using aforesaid relation value of c and φ is estimated for prepared specimens for both types of joints by plotting curve between σ_n and τ. The curve for Type I joint is shown in Fig. 4.38 while for Type II joint the plotted curve is shown in Fig. 4.39.

Best fitted linear curve is plot for the co ordinates obtained from experiments. Slope of the best fitted line gives the value of tanφ. Value of shear stress (τ) at zero normal stress (σ_n) gives the value of cohesion.

For Type I joint slope of the best fitted line is calculated as 1.0159 hence value of φ is estimated as 45.45°. The cohesion value was estimated as 0.0293 MPa. Hacksaw joint i.e. Type II joint has cohesion value of 0.058 MPa and slope of the best fitted linear curve was calculated as 0.866 corresponding to which value of φ is 40.88°.

CHAPTER 5
CONCLUSIONS

The work was carried out to study the stiffness characteristics for two types of roughness joints prepared in laboratory using Plaster of Paris. The specimens were studied under various normal stress values. The shear stiffness values were estimated by using the direct shear tests and the normal stiffness values were estimated by using the compressive strength test equipment. Then the following conclusions were made from the preceding work.

- The peak shear stress values of joints increases with normal stress values. Thus the shear stiffness value increases with normal stress which is in accordance with previous studies.
- Variation of shear stress with deformation was similar in both Type I (Natural) and Type II (Hacksaw) joints.
- The shear stress varies non linearly.
- Peak shear stiffness values for Type I (Natural) joints was higher than peak shear stiffness values for Type II (Hacksaw) joints.
- Values of Mohr- Coulomb shear parameters were found to be

  Type I (Natural) - $c = 0.0293$ MPa & $\varphi = 45.45°$

  Type II (Hacksaw) - $c = 0.0580$ MPa & $\varphi = 40.88°$

- Average Normal Stiffness values (MPa/mm) was found to be:

	Type I (Natural)	Type II (Hacksaw)
One Joint	2.28	2.22
Two Joints	1.58	4.17
Three Joints	1.23	3.70
Four Joints	0.69	3.65

- Average normal stiffness values for Type I (Natural) joints was lesser than average normal stiffness values for Type II (Hacksaw) joints.

- Average Normal Stiffness values follow a down trend with increasing number of joints.
- In all one, two, three and four discontinuities with Type I (Natural) joints undergoes more deformation as compared to Type II (Hacksaw) joints.
- Following empirical equations have been proposed to estimate the shear stiffness (k_s) of rock joints under any normal stress. (σ_n) conditions.

  Type I (Natural) -

$$k_s = a \times e^{b\sigma_n}$$

  Where, a = 0.0376

  b = 2.410

  Type II (Hacksaw)-

$$k_s = a' \times e^{b'\sigma_n}$$

  Where, a' = 0.04291

  b' = 2.201

  and hence the departure of Type II (Hacksaw) joint from Type I (Natural) joint can be given as

$$\frac{a}{a'} = 0.8763 \quad \text{and} \quad \frac{b}{b'} = 1.0950$$

- As the ratio of b/b' is almost equal to one it can be concluded that the shear stiffness of joints varies because of parameters a and a'
- Here ratio of a/ a' is not equal to one. This indicates that joints having different roughness profiles will have different values of a/ a', hence roughness profiles of joints influences the shear stiffness in jointed rock masses.

REFERENCES

1. **Bandis S.C., Lumsden A.C., Barton N.R.,** (1983), "Fundamentals of rock joint deformation", *International Journal of Rock Mechanics and Mining Sciences & Geomechanics Abstracts*, 20 (6), 249-268.

2. **Barton N.R.,** (1972), **"**A model study of rock-joint deformation", *International Journal of Rock Mechanics and Mining Sciences & Geomechanics Abstracts*, 9 (5), 579-582.

3. **Barton N.R**., (1975), "A review of the shear strength of field discontinuities in rock", *International Journal of Rock Mechanics and Mining Sciences & Geomechanics Abstracts*, 12 (4), 55-56.

4. **Barton N.,** (1976), **"**The shear strength of rock and rock joints", *International Journal of Rock Mechanics and Mining Science & Geomechanics Abstracts*, 13 (9), 255-279.

5. **Barton N., Bandis S.,** (1980**),** "Some effects of scale on the shear strength of joints", *International Journal of Rock Mechanics and Mining Sciences & Geomechanics Abstracts*, 17 (1), 69-73.

6. **Barton N., Choubey V.,** (1977), "The shear strength of rock joints in theory and practice", *Rock Mechanics and Rock Engineering*, 10, 1-54.

7. **Bill F.G,** "Engineering properties of soils and rocks", Fourth edition, Blackwell Science Publication.

8. **Goodman R. E.,** (1989), Introduction to Rock Mechanics, second edition, John Wiley & Sons. USA.

9. **Haberfield C.M, Seidel J.P,** (1999), “Some recent advances in the modelling of soft rock joints in direct shear”, *Geotechnical and Geological Engineering*, 17, 177-195.

10. **Hsiung S. M., Ghosh A., Ahola M.P., Chowdhury A.H.,** (1993), “Assessment of conventional methodologies for joint roughness coefficient determination” *International Journal of Rock Mechanics and Mining Sciences & Geomechanics Abstracts*, 30 (7), 825-829.

11. **Huang S. L., Oelfke S.M., Speck R.C.** (1992), “Applicability of fractal characterization and modelling to rock joint profiles” *International Journal of Rock Mechanics and Mining Sciences & Geomechanics Abstracts*, 29 (2), 89-98.

12. **Indraratna B., Haque A., Aziz N.,** (1998), “Laboratory modelling of shear behaviour of soft joints under constant normal stiffness conditions”, *Geotechnical and Geological Engineering”*,16, 17-44.

13. **Indraratna B, Hauqe A**, (1997), “Experimental study of shear behaviour of rock joints under constant normal stiffness conditions.”, *International Journal of Rock Mechanics and Mining Sciences*, 34 (141),

14. **IS 2720 (PART XIII)**, (1986). “Direct shear test”.

15. **Jiang X. W, Wan Li, Wang Xu-Sheng, Liang Si-Hai, Hu Bill X,** (2009) “Estimation of fracture normal stiffness using a transmissivity-depth correlation”, *International Journal of Rock Mechanics and Mining Sciences*, 46(1), 51-58.

16. **Jiang Y, Xiao J, Tanabashi Y, Mizokami T**, (2004), “Development of an automated servo-controlled direct shear apparatus applying a constant normal stiffness condition.” *International Journal of Rock Mechanics and Mining Sciences*, 41, 275-286.

17. **Lee Y. H., Carr J. R., Barr D.J., Haas C.J.,** (1990), “The fractal dimension as a measure of the roughness of rock discontinuity profiles”, *International Journal of*

Rock Mechanics and Mining Sciences & Geomechanics Abstracts, 27 (6), 453-464.

18. **Marrapu Deepa,** (2008), "Stiffness characteristics of rock joints under low to high normal loads", M.Tech Thesis, IIT Delhi, India.

19. **Pratt H.R., Black A.D., Brown W.S., Brace W.F.,** (1972), "The effect of specimen size on the mechanical properties of unjointed diorite", *International Journal of Rock Mechanics and Mining Sciences & Geomechanics Abstracts*, 9 (4), 513-516.

20. **Seidel J. P., Haberfield C.M.,** (2002), "A theoretical model for rock joints subjected to constant normal stiffness direct shear" *International Journal of Rock Mechanics and Mining Sciences*, 39 (5), 539-553, (2002).

21. **Singh R.N, Ghosh A.K,** (2006) "Engineered rock structures in mining and civil construction", Taylor and Francis, London.

22. **Tse R., Cruden D.M.,** (1979), "Estimating joint roughness coefficients" *International Journal of Rock Mechanics and Mining Sciences & Geomechanics Abstracts*, 16 (5), 303-307.

23. **Wines D.R, Lilly P.A.**, (2003), "Estimates of rock joints shear strength in part of the Fimiston open pit operation in Western Australia", *International Journal of Rock Mechanics and Mining Sciences,* 40, 929-937.

24. **Yoshinaka R, Yamabe T.,** (1986), "Joint stiffness and the deformation behaviour of discontinuous rock" *International Journal of Rock Mechanics and Mining Science & Geomechanics Abstracts*, 23 (1), 19-28.